R. & M. No. 3009
(15,972)
A.R.C. Technical Report

MINISTRY OF SUPPLY

AERONAUTICAL RESEARCH COUNCIL
REPORTS AND MEMORANDA

Low-speed Wind-Tunnel Measurements of Longitudinal Oscillatory Derivatives on Three Wing Plan-forms

By

G. F. Moss, B.Sc.

LONDON : HER MAJESTY'S STATIONERY OFFICE
1957
TEN SHILLINGS NET

Low-speed Wind-Tunnel Measurements of Longitudinal Oscillatory Derivatives on Three Wing Plan-forms

By

G. F. Moss, B.Sc.

Communicated By the Principal Director of Scientific Research (Air), Ministry of Supply

Reports and Memoranda No. 3009*

November, 1952

Summary.—Tests have been made on a 90-deg apex delta wing, a 60-deg swept-back wing and a 40-deg swept-back wing to obtain values of longitudinal oscillatory derivatives for various frequencies, amplitudes and Reynolds numbers. Values of $m_{\dot\theta}$ were obtained for all three models and z_w for the delta model using free oscillation methods. In addition, z_θ, $z_{\dot\theta}$, m_θ and $m_{\dot\theta}$ were measured by a forced oscillation method for the delta wing and the 60-deg swept-back wing.

The effects of reduced frequency (over the range $0 \cdot 01$ to $0 \cdot 3$), amplitude ($\pm \frac{1}{2}$ deg to ± 2 deg in pitch) and Reynolds number ($0 \cdot 72 \times 10^6$ to $3 \cdot 3 \times 10^6$) were found to be small.

1. *Introduction.*—Flight experience on some of the latest aircraft prototypes has shown a reduction of pitching damping in the short-period oscillation at high speeds. Tunnel measurements of the oscillatory derivatives involved (eight in all) have in the past been mainly limited to the most important one (and only recently have these been made at high subsonic Mach numbers[1,2,3]). Theory[4] shows that to predict the oscillatory behaviour of an aircraft the values of all eight derivatives are needed. The minimum requirement for a wind-tunnel experiment to obtain this information is a test giving lift and pitching-moment coefficients of stiffness and damping at each of two axes of oscillation. The required number of measurements were made in these tests, but the accuracy, although by no means poor, was not sufficient to extract the basic derivatives from the ill-conditioned simultaneous equations which it is necessary to solve (for structural reasons the axes of oscillation were relatively close together).

The experimental technique is new and it may be some time before an entirely satisfactory experimental procedure is established. Work on these lines is proceeding both at the Royal Aircraft Establishment[5] and the National Physical Laboratory in high-speed wind tunnels.

The value of low-speed wind-tunnel measurements of these derivatives lies in the help given to theoretical work[6,7,8]. A first attempt was made using a resonance method with only limited success[9]. The present report gives the results of further tests on three typical wing plan-forms using two distinct experimental methods. First, values of z_θ, $z_{\dot\theta}$, m_θ and $m_{\dot\theta}$ each at two axes of oscillation (*i.e.*, all the derivatives required for a complete analysis) were measured using a forced-oscillation method. The damping coefficients $z_{\dot\theta}$ and $m_{\dot\theta}$ could not be measured accurately using this experimental method and a free-oscillation method (in which damping causes a more readily measurable effect) was devised to give more accurate values of $m_{\dot\theta}$. No similar method

* R.A.E. Tech. Note Aero. 2208—received 5th June, 1953.

for $z_{\dot{\theta}}$ was found possible. The forced-oscillation values of $z_{\dot{\theta}}$ were not accurate enough to enable calculation of $z_{\dot{w}}$ and a further free-oscillation rig was designed to measure $z_{\dot{w}}$ directly for the delta-wing plan-form.

2. *Experimental Methods*.—2.1.—*General*.—The tests were made between June, 1951 and July, 1952 in the No. 2 $11\frac{1}{2}$-ft $\times$ $8\frac{1}{2}$-ft Low-Speed Wind Tunnel of the Royal Aircraft Establishment, Farnborough, at wind speeds of 101, 201, and 290 ft/sec. Three plan-forms were tested as follows:

TABLE A

	90-deg delta wing	60-deg swept wing	40-deg swept wing
Sweepback on quarter-chord line	36·9°	60°	40°
Aspect ratio	3·02	3	4·4
Taper ratio	0·143	—	0·311
Thickness/chord ratio	10%	{ 6% inboard 12% at tips }	10%

Two models of the 90-deg delta-wing plan-form were used, one with a removable body and one with no body 0·61 the size of the first. Two models of the 40-deg swept wing were also tested, one with and one without a body and fin; the model with body was 0·88 the size of the other. Only one model of the 60-deg swept wing was used; there was no provision made for removing the body in this case. Full details of the models are given in Table 1 and Figs. 1, 2, 3 and 4.

The programme of tests was as follows:

TABLE B

	Measured by forced oscillations in pitch	Measured by free oscillations in pitch	Measured by free heaving oscillations
5·485 ft span 90° delta wing with removable body	z_θ, $z_{\dot{\theta}}$, m_θ, $m_{\dot{\theta}}$ Two axes of oscillation Amplitude $= \pm 1{\cdot}65°$ With body only	$m_{\dot{\theta}}$ Two axes of oscillation Amplitudes $= \pm \frac{1}{2}°$ $\pm 1° \pm 1\frac{1}{2}° \pm 2°$ With and without body	z_w Amplitudes $\pm 4{\cdot}56\%\bar{c}$ and $\pm 9{\cdot}12\%\bar{c}$ With and without body
3·35 ft span 90° delta wing; no body	—	$m_{\dot{\theta}}$ Two axes of oscillation Amplitudes $= \pm 1° \pm 2°$	—
60° swept-back wing with body	z_θ, $z_{\dot{\theta}}$, m_θ, $m_{\dot{\theta}}$ Two axes of oscillation Amplitude $= \pm 1{\cdot}70°$	$m_{\dot{\theta}}$ Two axes of oscillation Amplitudes $= \pm \frac{1}{2}°$ $\pm 1° \pm 1\frac{1}{2}° \pm 2°$	—
40° swept-back wing; no body ..	—	$m_{\dot{\theta}}$ Three axes of oscillation Amplitudes $= \pm 1° \pm 2°$	—
40° swept-back wing with body ..	—	$m_{\dot{\theta}}$ Two axes of oscillation Amplitudes $= \pm \frac{1}{2}°$ $\pm 1° \pm 1\frac{1}{2}° \pm 2°$	—

All these tests were made at a mean incidence of zero, but some extra values of $m_{\dot\theta}$ were measured over an incidence range for the 5·485 span 90-deg delta wing without body, using the free-oscillation method.

For the oscillations in pitch, the model was supported on two forward struts by means of cross-spring pivots inside the wing and was oscillated about this position by means of a rear strut attached to a rigid sting bolted to the model. This attachment was in the form of another cross-spring pivot which could have any desired position along the sting. Two pivot positions were provided on each model except the 40-deg swept wing with no body where three were provided. In order to made an accurate analysis of the result it is essential that the pivot positions should be as far apart as possible, but in these tests this distance was limited by considerations of model strength. One pivot position was placed near the aerodynamic centre in each case:

TABLE C

	90-deg delta wing (both models)	60-deg swept wing	40-deg swept wing no body	40-deg swept wing with body
Aerodynamic centre	$0 \cdot 315\bar{c}$	$0 \cdot 340\bar{c}$	$0 \cdot 320\bar{c}$	$0 \cdot 330\bar{c}$
Axes of oscillation	$0 \cdot 328\bar{c}$ $0 \cdot 055\bar{c}$	$0 \cdot 288\bar{c}$ $0 \cdot 0\bar{c}$	$0 \cdot 258\bar{c}$ $-0 \cdot 051\bar{c}$ $0 \cdot 572\bar{c}$	$0 \cdot 258\bar{c}$ $-0 \cdot 051\bar{c}$

2.2. *Method of Inexorable Forcing* (*Figs.* 5, 6 *and* 7).—The oscillatory motion of the model about the pivot in the wings was inexorably forced by the rear strut which was attached at the lower end to a flywheel and crank. Measurement was made of the oscillatory forces in the forward support struts and the rear strut by means of wire-resistance strain-gauges. The model inertia forces in the forward struts, which would have swamped the aerodynamic forces, were made very nearly zero by arranging the distribution of mass in the model to be such that the forward struts were approximately at the ' centre of percussion ' of the system. A somewhat complicated system was used to counteract the model inertia forces in the rear strut. The ' balance ' used is shown in Fig. 6. The rear strut was connected to the end B of a beam BC pivoted to earth at C. The forcing crank was connected to the beam BC near to B at A. The force in the rear strut was measured by measuring the reaction at the pivot C. This was done by carrying the pivot C on strain-gauged strips, E. Solid friction was eliminated by using cross-spring pivots throughout. A suitable mass M clamped to the beam BC between A and C compensated the model inertia forces in the rear strut measured at E and the spring S made the effect of any spring stiffnesses zero. The dead weight of the model was taken by a support spring above the tunnel and care was taken to use the full range of strain permissible in the strain-gauged strips E. These were $\frac{1}{2}$-in. wide and 0·003 in. thick and were strained up to 650×10^{-6}* for the maximum pitching-moment stiffness encountered (*i.e.*, $\pm$ 20 lb in the rear strut). The corresponding damping component in this instance was a strain of 8×10^{-6}, but in some cases strains as low as 4×10^{-6} were measured. The electrical circuit was able to detect $0 \cdot 2 \times 10^{-6}$ strain and so the measurements of $m_{\dot\theta}$ were accurate to 5 per cent; the accuracy in the readings of m_θ was much better. Similar accuracies were obtained on the lift forces in the forward struts.

The electrical circuit is shown in Fig. 7. The strain-gauges were arranged in a simple bridge on each pick-up. Two opposite corners of each bridge were provided with power and the potential across the other two corners was kept zero by means of a graduated helical potentiometer and a sensitive mirror galvanometer. The power to the gauge bridges was of square-wave form, the switching contacts being operated by a cam on the forcing crankshaft. Appendix I shows that by using two square waves in turn, one being ' in phase ' with the forcing motion and one ' in

* Considered a maximum for accurate strain-gauge work.

quadrature ', the mean signals balanced by the potentiometer are proportional to the ' in phase ' and ' in quadrature ' components of strain respectively, and thus to the stiffness and the damping forces in the strained member. Care was taken that the mean levels of the square waves themselves were zero, since any standing potential would have caused a deflection on the galvanometer. This was checked before each reading and adjustment, if required, was made by altering the height of the square wave (C_1 and C_2). As described in Appendix I, the switching of the square wave was made $\pi/6$ late on the ' make ' and $\pi/6$ early on the ' break ' points in order to remove the effect of any third harmonic in the model motion. The effect of all even harmonics was automatically zero, so the lowest harmonic able to cause error was the fifth. The motion was later photographed under various conditions of load and found to be virtually free of all harmonics.

The effect of thermo-electric currents was removed by reversing the battery leads at every reading and taking a mean in the usual way.

The apparatus was calibrated by applying springs of known stiffness to the sting of the model, the damping of these being assumed to be zero.

The values of z_θ and m_θ at zero frequency included in the tables and figures were measured by using the usual tunnel balance on which the model and forcing mechanism were mounted.

2.3. *Method of Free Oscillations.*—2.3.1. *Pitching oscillations* (*Figs. 8 and 9*).—The models were mounted on two forward struts as before, but the rear strut from the model sting was pivoted to one side of a rocking beam above the tunnel. A long pointer fixed to the rocking beam recorded the oscillatory motion of the model on a revolving drum, the trace being made by sparking through Teledeltas paper. The spring S_2 supported the model dead load. The natural frequency of the apparatus could be made small by clamping weights in the compartments at the extremities of the rocking beam, and made large by attaching the springs S_1. In this way a range of periodic time from about 5 seconds down to about 0·4 seconds was obtained, giving a range of reduced frequency from approximately 0·01 (at $V = 290$ ft/sec) to 0·3 (at $V = 101$ ft/sec).

The experiment consisted of recording the decay of oscillation with time after an initial displacement of $2\frac{1}{2}$ deg of model incidence. From this, values of $m_{\dot{\theta}}$ were calculated at various amplitudes down to $\pm\frac{1}{2}$ deg (*see* Appendix II). The value of the apparatus damping (no wind) was obtained before each wind-on measurement; the values of $m_{\dot{\theta}}$ given in the tables were computed by adding to the difference between these two the still-air damping obtained by separate experiment (*see* section 3). All pivots in the apparatus were in the form of cross-spring bearings so the only solid friction was that of the pen on the recording drum. This was made very small (equivalent to $\Delta m_{\dot{\theta}} \simeq 0\cdot0006$ at $V = 101$ ft/sec) and in any case was unaffected by aerodynamic loads and thus disappeared in the subtraction of wind-off from wind-on readings. The apparatus damping itself increased consistently with the addition of springs or weights to the rocking beam. This was presumably due to the increased stress in the cross-spring pivots supporting the beam.

The aerodynamic stiffness ceofficient m_θ theoretically could have been derived from the measured difference in periodic time due to the wind. Unfortunately, it was only possible to measure the periodic time to an accuracy of about 0·005 seconds (although a very accurate stop watch was used) because the oscillations with the wind on decayed too quickly. An accuracy of about 0·0001 seconds in periodic time would have been required to give m_θ to 2 or 3 per cent.

2.3.2. *Heaving oscillations* (*Figs. 10 and 11*).—The model was constrained to move vertically by two parallel link frames pivoted to the tunnel structure. The steel column on which the model hung consisted of a thin steel web bolted to a girder; the web was bolted to the model at the lower end and the girder was pivoted to the ends of the link frames. The rocking beam used previously (section 2.3.1) was used to record the vertical oscillations of the model by means of a short connecting rod to the lower link frame. The weight of the model and steel column was taken by a large number of short support springs, S, arranged in series. The number of these springs used determined the frequency of oscillation, but some extra control on frequency was obtained in some cases by the use of springs and weights on the rocking beam. A range of periodic time from $2 \cdot 3$ seconds down to $0 \cdot 6$ seconds was thus obtained, giving a range of reduced frequency from $0 \cdot 025$ (at $V = 201$ ft/sec) to $0 \cdot 18$ (at $V = 101$ ft/sec). The weight of model and support column and the strength of the support spring were considerable ; it was found necessary to use a winch and a bomb-release mechanism to set the system in oscillation.

The experiment consisted of recording the decay of vertical oscillation of the model after an initial displacement of $2\frac{1}{2}$ in. The damping coefficient z_w was calculated at two amplitudes $\pm$ 2 in. $\pm$ 1 in. (*i.e.*, $\pm$ $9 \cdot 12$ and $\pm$ $4 \cdot 56$ per cent mean chord) by the method given in Appendix II. The apparatus damping (no-wind) was obtained before and after each wind-on measurement; the quoted values of z_w were computed by subtracting the mean of these two no-wind values from that obtained with wind on. As before, all pivots in the system were in the form of springs or cross-springs, the only solid friction being that of the recording pen. The damping of the apparatus itself was small and remained sensibly constant over the period of the tests.

No difference in periodic time due to the wind was observed above the limits of experimental error.

2.4. *Sources of Experimental Error.*—2.4.1. *Fluctuations in the tunnel stream.*—The presence of incidence fluctuations in the tunnel stream having a frequency below about 10 cycles/sec could have affected the measurements. To check that no such fluctuations were present, the larger delta wing was clamped at zero incidence and the variation of lift force with time recorded electronically using the strain-gauges on the forward support strut. No fluctuations were apparent, although the apparatus was sensitive to $\pm$ $0 \cdot 05$ deg of incidence.

2.4.2. *Internal damping of the cross-spring pivots.*—The cross-spring pivots in some cases were subject to aerodynamic loads which affected their stiffness and internal damping. In general the loads were very small for the size of pivot, but in the case of the forward strut pivots large oscillating lift forces were taken. A bench test showed that under these conditions the changes in damping and stiffness of the pivot were small ; equivalent to an error of $0 \cdot 0003$ on $m_{\dot{\theta}}$ and $0 \cdot 00002$ on m_θ for the most severe case.

2.4.3. *Harmonics in the model motion.*—In the tests using the method of inexorable forcing, the presence of odd harmonics above and including the fifth would have caused errors in the measurements (Appendix I). The model motion was photographed by a high-speed camera under various conditions of load. No difference from the true sinusoidal motion could be detected.

2.4.4. *The effect of rate of decay in the model motion.*—In the tests with free oscillations the damping depended on the product of effective model inertia and the rate of decay in the model motion. The frequency was sometimes changed by altering spring stiffness and sometimes by altering the inertia. In the former, the effect of frequency was measured directly, inertia and rate of decay being approximately constant, but in the latter the change in frequency occurred along with a change in rate of decay. To check that the effect of change in rate of decay was negligible, an experiment was repeated with no change of frequency but with a large change in inertia and thus in rate of decay. The same damping was recorded showing that this effect was either zero or negligible.

3. *Corrections Applied.*—Normal static tunnel constraint corrections to pitching amplitude and pitching moment have been applied to the results obtained with the inexorable forcing method ; the corrections for oscillating wings of finite span are not yet known. No corrections have been applied to the free-oscillation values of $m_{\dot{\theta}}$. The normal static tunnel correction has also been applied to the measured values of z_w, since the heaving oscillation causes oscillating angles of incidence subject to tunnel constraint. These corrections were calculated from Ref. 10 and were applied to the results over the whole frequency range. The correction to all derivatives on

account of angle of pitch was + 4 per cent for the delta wing and + 3 per cent for the 60 deg swept wing. The pitching-moment corrections were + 0·001 and + 0·005 on m_θ for the two models respectively ; the correction to $m_{\dot\theta}$ on account of pitching moment was negligible.

The discrepancy between the measured values of $m_{\dot\theta}$ for the two sizes of delta model is small and may be mainly due to the larger strut interference on the smaller model where the size of the strut heads was comparatively large (Fig. 18). The present results for the larger delta model agree well with those in Refs. 1 and 2 where quite different ratios of model size to tunnel size were used (Fig. 26). The general indication appears to be that the tunnel constraint corrections for these results must be small, with the possible exception of the 40-deg swept-back wing models where the wing tips were comparatively near the tunnel walls.

In both experimental methods the still-air value of $m_{\dot\theta}$ was lost in the subtraction of the no-wind damping from the wind-on damping. The value of the still-air $m_{\dot\theta}$ was measured separately by a simple free-oscillation method and was added to the results (equivalent to about $1\frac{1}{2}$ per cent at 200 ft/sec). No still-air damping was measured for the z_w tests, so the quoted values will be slightly low on this account. The values of $z_{\dot\theta}$ are also uncorrected for still-air effects.

4. *Results*.—The values of z_θ, $z_{\dot\theta}$, m_θ and $m_{\dot\theta}$ obtained by the method of inexorable forcing are given in Table 2 and Figs. 12 to 15 inclusive, and the values of $m_{\dot\theta}$ obtained by the free-oscillation method in Tables 3 to 7 inclusive and Figs. 16 to 24 inclusive. The measurements of z_w for the larger delta wing are given in Table 8 and Fig. 25.

In general the effects of frequency and amplitude were small over the range of investigation. The values of m_θ and $m_{\dot\theta}$, however, for the 60-deg swept wing showed a tendency to become more negative with increase of frequency at the forward axis of oscillation (Fig. 15). There was also some marked scale effect present. The comparison between the values of $m_{\dot\theta}$ obtained by the two experimental methods is shown in Fig. 13 for the 90-deg delta wing and in Fig. 15 for the 60-deg swept wing. Of the two methods the free-oscillation method was far more accurate, but there was fair agreement in the values of $m_{\dot\theta}$ obtained at the rearmost axis position on both models and a consistent difference at the forward axis position. A possible explanation of this is that the unknown tunnel corrections to damping may be different for the two methods and dependent on axis position[11]. The difference in $m_{\dot\theta}$ for the delta model (Fig. 13) is too large to be entirely explained in this way, however, since tunnel corrections are believed to be small (*see* section 3).

Theoretical derivatives for the delta wing are plotted in Figs. 12 and 13[6,7]. The low values of reduced frequency applicable to stability work make theoretical estimation less difficult. The theoretical values of $z_{\dot\theta}$ and $m_{\dot\theta}$ are more negative than the measured values, but there is good agreement both with the actual values of z_θ and m_θ and with the small frequency effect on all four derivatives.

In the results obtained with free oscillations there was a small variation in $m_{\dot\theta}$ at low reduced frequency. The reason for this is obscure. The comparison between the measurements for the two delta-wing models (Fig. 18) shows that there is a tendency for this variation to occur at smaller frequencies on the smaller model. Also, in most cases, the slight reduction in damping occurs when the tunnel return circuit contains a whole number of wavelengths of the motion, *i.e.*, when disturbances travelling round the tunnel circuit could be expected to reinforce the motion. The possibility of such periodic disturbances travelling through the fan and screens seems doubtful, but whatever the explanation, it seems probable that the phenomenon is due to tunnel effects.

The comparison between $m_{\dot\theta}$ obtained on the two delta models is shown in Fig. 18. The larger damping obtained on the small model cannot be due to a difference in Reynolds number, since the Reynolds number ranges for the two models overlapped. The difference in tunnel correction should be small (section 3). The discrepancy may be mainly due to the increased strut interference on the smaller model. The same size of strut heads was used in the two cases and the pivots protruded a little from the lower wing surface of the smaller model because the wing was thinner.

The measurements of damping in pitch for the 90-deg delta wing at mean incidences up to $\alpha = 15$ deg are shown in Fig. 19. There was little change up to about $\alpha = 8$ deg when the first unsteadiness of flow was apparent at the wing tips, but at higher incidences there was a rapid increase in damping associated with the inboard spread of the tip stall.

The results for the 40-deg swept-back wing with no body are shown in Fig. 24. On all the models tested the scale effect on $m_{\dot{\theta}}$ increased with distance of the axis of oscillation from the neutral point. The scale effect on the 40-deg swept-back wing was considerable and made analysis difficult. Comparison between the results for the two models shows agreement for the $0 \cdot 258\bar{c}$ axis position, but a large difference at the $- 0 \cdot 051\bar{c}$ axis position. The effect of the body cannot have been so great as this in view of the small body effect found on the delta-wing plan-form at both axis positions. Both 40-deg swept-back wing models were large, the model without body being a little larger than the model with body and it is possible, therefore, that the effect of tunnel constraint (the corrections for oscillating models of finite span are not yet known) may have contributed to the discrepancy in measured damping.

The values of z_w obtained on the larger delta-wing model are shown in Fig. 25. No effect of amplitude or frequency was found over the range investigated. The body contribution to the damping was approximately 4 per cent of the total.

Curves of $m_{\dot{\theta}}$ against ' axis of oscillation ' position for the three plan-forms are shown in Fig. 26. The calculations were made using the equations of Ref. 4 with the static values of z_w (*i.e.*, assuming no variation of z_w with frequency). Experimental values for the delta plan-form from Refs. 1 and 2, and theoretical values from Ref. 7 are also plotted in the figure and agree well with the present tests.

The small distance apart of the axis positions, fixed by considerations of model strength, and the inaccuracy in the measurement of $z_{\dot{\theta}}$ inherent in the experimental method, have made any complete analysis impossible.

5. *Conclusions*.—On all the derivatives measured there appeared to be only small effects of frequency and amplitude and the additional damping due to a body was also small in both pitching and heaving.

NOTATION

S	Wing area
$\bar{c}$	Wing geometric mean chord
ρ	Air density
V	Wind speed
w	Heaving velocity
f	Frequency of oscillation
ω	$= \dfrac{2\pi f \bar{c}}{V}$ Reduced frequency
α	Static mean incidence
θ	Amplitude of oscillatory angle of pitching (to fixed axes)

NOTATION—*continued*

$$z_{\theta} = \frac{Z_{\theta}}{\rho S V^2}$$

$$z_{\dot{\theta}} = \frac{Z_{\dot{\theta}}}{\rho S V \bar{c}}$$

$$z_w = \frac{Z_w}{\rho S V}$$

$$z_{\dot{w}} = \frac{Z_{\dot{w}}}{\rho S \bar{c}}$$

$$m_{\theta} = \frac{M_{\theta}}{\rho S V^2 \bar{c}}$$

$$m_{\dot{\theta}} = \frac{M_{\dot{\theta}}}{\rho S V \bar{c}^2}$$

$$m_w = \frac{M_w}{\rho S V \bar{c}}$$

$$m_{\dot{w}} = \frac{M_{\dot{w}}}{\rho S \bar{c}^2}$$

REFERENCES

No.	*Author*	*Title, etc.*
1	J. B. Bratt, W. G. Rayner and R. Cartwright.	Measurement of the direct pitching moment derivatives for a delta wing at high subsonic speeds. A.R.C. 13,866. March, 1951.
2	M. Tobak, D. E. Reese and B. H. Beam.	Experimental damping in pitch of a 45-deg triangular wing. N.A.C.A. Research Memo. A50J26. A.R.C. 14,438. December, 1950.
3	J. B. Bratt, W. G. Rayner and J. E. G. Townsend.	Measurements of the direct pitching moment derivatives for an English Electric transonic wing at high subsonic speeds. A.R.C. 14,301. October, 1951.
4	S. Neumark and A. W. Thorpe ..	Theoretical requirements of tunnel experiments for determining stability derivatives in oscillatory longitudinal disturbances. R.A.E. Tech. Note Aero. 2059. A.R.C. 13,667. June, 1950.
5	L. H. G. Sterne	A proposed apparatus for measuring oscillatory aerodynamic derivatives. R.A.E. Tech. Memo. Aero. 167. March, 1951. A.R.C. 14,227.
6	D. E. Lehrian	Aerodynamic coefficients for an oscillating delta wing. R. & M. 2841. July, 1951.
7	D. E. Lehrian	Calculation of stability derivatives for oscillating wings. R. & M. 2922. February, 1953.
8	W. P. Jones..	Oscillating wings in compressible subsonic flow. R. & M. 2855. October, 1951.
9	G. F. Moss	Some low speed wind tunnel measurements of damping in pitch for a delta wing. R.A.E. Tech. Memo. Aero. 123. November, 1950.
10	W. E. A. Acum	Corrections for symmetrical swept and tapered wings in rectangular wind tunnels. A.R.C. 14,159. July, 1951.
11	W. P. Jones..	Wind tunnel interference effects on measurements of aerodynamic coefficients for oscillating aerofoils. R. & M. 2786. September, 1950.

APPENDIX I

Method of Inexorable Forcing—Measurement of Forces

It was required to measure the amplitude and phase of the oscillatory aerodynamic force in the model supports. The principle used was to supply strain-gauges on the supports with an alternating voltage synchronous with the motion of the model. This voltage could have been produced by an alternator geared to the forcing crankshaft[5], but since the speed of rotation was low and the forcing motion could be assumed free of harmonics, a square-wave form of alternating voltage was used. This was produced by a simple cam and had the advantage of giving a constant voltage at all rotational speeds. It was found to be mechanically convenient to allow a small interval between the positive and negative loops of the square-wave voltage and this interval was made equal to $\pi/3$ as an extra safeguard against error from any third harmonic in the forcing motion (subsequently the motion was proved to be virtually free of all harmonics—section 2.4.3).

To calculate the output from the gauges when fed with this signal, let the strain in the gauged member be

$$S \sin (\Omega t + \phi) .$$

If the supply voltage to the gauge bridge is a square wave of the form:

$+ E$ volts for the interval $\pi/6$ to $5\pi/6$, etc.

and $- E$,, ,, ,, ,, $7\pi/6$ to $11\pi/6$, etc.

the signal from the gauges is given by the product of the strain and the applied voltage; *i.e.*, it has a mean value:

$$\frac{1}{\pi}\int_{\pi/6}^{5\pi/6} (+ E)S \sin (\Omega t + \phi)\, d(\Omega t) + \frac{1}{\pi}\int_{7\pi/6}^{11\pi/6} (- E)S \sin (\Omega t + \phi)\, d(\Omega t).$$

This simplifies to

$$\frac{4 \cos \pi/6}{\pi} ES \cos \phi .$$

Thus the mean value of the signal is proportional to the 'in phase' component of the strain.

In a similar way by using a square wave of the form:

$+ E$ volts for the interval $- \pi/3$ to $+ \pi/3$, etc.

and $- E$ volts ,, ,, ,, $2\pi/3$ to $4\pi/3$, etc.

a signal is obtained with a mean value of

$$\frac{4 \cos \pi/6}{\pi} E\, S \sin \phi$$

being proportional to the 'in quadrature' component of the strain.

The effect of a third harmonic in the oscillatory motion is zero, since any component of strain of the form $\sin 3\Omega t$ leads to a zero mean value in the resulting signal.

APPENDIX II

Calculation of Damping by Method of Free Oscillations

The equation of motion for free pitching oscillations is of the form:

$$I\ddot{\theta} - M_{\dot{\theta}}\dot{\theta} + K\theta = 0$$

where I is the moment of inertia of the model.

The solution of this equation is of the form:

$$\theta = A\, e^{-\lambda t} \sin(nt + \varepsilon)$$

where $\lambda = -\dfrac{M_{\dot\theta}}{2I}$.

Thus if the amplitude of oscillation is θ_1 at time t_1 and θ_2 at time t_2:

$$\frac{\theta_1}{\theta_2} = e^{\lambda(t_2 - t_1)}$$

or

$$\lambda = \log \frac{\theta_1/\theta_2}{t_2 - t_1}$$

or

$$M_{\dot\theta} = -\frac{2I \log(\theta_1/\theta_2)}{t_2 - t_1}.$$

Similarly in the case of heaving motion if the amplitude of oscillation is δ_1 at time t_1 and δ_2 at time t_2:

$$Z_w = -\frac{2M \log(\delta_1/\delta_2)}{t_2 - t_1}$$

where M is the mass of the model.

TABLE 1

Model Data

	5·485-ft span 90-deg delta wing	3·35-ft span 90-deg delta wing	60-deg swept wing	40-deg swept wing model with body	40-deg swept wing model without body
Wing					
Area (sq ft)	10·029	3·783	9·50	13·09	14·948
Span (ft)	5·485	3·350	5·33	7·60	8·124
Mean chord (ft)	1·828	1·129	1·780	1·722	1·840
Thickness/chord ratio (per cent) ..	10	10	6	10	10
Section	RAE102	RAE102	RAE101	E.Q. 10.40	E.Q. 10.40
Apex angle (deg)	90	90	60	92·46	92·46
Sweepback of quarterchord line (deg)	36·9	36·9	60	40	40
Centre-line chord (ft)	3·200	1·967	2·250	2·627	2·806
Tip chord (ft)	0·457	0·292	0·169	0·817	0·873
Taper ratio	0·143	0·143	—	0·311	0·311
Aspect ratio	3·00	2·97	3	4·4	4·4
Body		None			None
Length (ft)	5·75		6·75	4·70	
Maximum diameter (ft)	0·90		0·58	0·95	
Distance of nose from leading-edge centre-line wing chord (ft) ..	0·98		0·83	0·4	
Shape	aerofoil shaped		parallel	faired shape	
Mean quarter-chord point					
Back from apex (ft)	1·572	0·968	2·433	1·973	2·107
Pivot positions					
Per cent mean chord	5·5 32·8	5·5 32·8	0·0 28·8	−5·1 25·8	−5·1 25·8 57·2
Per cent centre-line chord ..	38·0 53·6	38·0 53·6	88·4 111·1	55·3 75·6	55·3 75·6 96·2

TABLE 2

Results Obtained by Method of Inexorable Forcing

(α_{mean} = 0 deg)

V (ft/sec)	ω	f (c.p.s.)	Amplitude (deg)	z_θ	$z_{\dot\theta}$	m_θ	$m_{\dot\theta}$
5·485-ft span 90-deg delta wing (with body): axis of oscillation at 0·055$\bar{c}$							
201	0	0	±1·65	−1·434	—	−0·374	—
201	0·031	0·55	±1·65	−1·414	−1·308	−0·361	−0·546
201	0·0785	1·38	±1·65	−1·424	−1·096	−0·373	−0·574
201	0·125	2·20	±1·65	−1·434	−1·125	−0·377	−0·582
201	0·168	2·97	±1·65	−1·414	−1·081	−0·374	−0·582
290	0	0	±1·65	−1·474	—	−0·385	—
290	0·0215	0·55	±1·65	−1·439	−1·135	−0·373	−0·466
290	0·0545	1·38	±1·65	−1·449	−1·244	−0·381	−0·564
290	0·0865	2·20	±1·65	−1·454	−1·135	−0·393	−0·573
290	0·117	2·97	±1·65	−1·464	−1·140	−0·390	−0·579
5·485 ft span 90-deg delta wing (with body): axis of oscillation at 0·328$\bar{c}$							
201	0	0	±1·645	−1·445	—	+0·026	—
201	0·031	0·55	±1·645	−1·445	−0·853	0·027	−0·326
201	0·0785	1·38	±1·645	−1·418	−0·869	0·025	−0·320
201	0·125	2·20	±1·645	−1·418	−0·875	0·026	−0·319
201	0·168	2·97	±1·645	−1·408	−0·848	0·026	−0·352
290	0	0	±1·645	−1·491	—	0·025	—
290	0·0215	0·55	±1·645	−1·454	−0·675	0·027	−0·323
290	0·0545	1·38	±1·645	−1·445	−0·787	0·025	−0·302
290	0·0865	2·20	±1·645	−1·436	−0·847	0·026	−0·350
290	0·117	2·97	±1·645	−1·445	−0·905	+0·026	−0·387
60-deg swept-back wing: axis of oscillation at 0·0$\bar{c}$							
201	0	0	±1·70	−1·172	—	−0·375	—
201	0·0305	0·55	±1·70	−1·133	—	−0·378	−0·707
201	0·0765	1·38	±1·70	−1·124	−1·160	−0·378	−0·610
201	0·122	2·20	±1·70	−1·152	−0·948	−0·396	−0·617
201	0·165	2·97	±1·70	−1·162	−1·104	−0·428	−0·652
290	0	0	±1·70	−1·179	—	−0·378	—
290	0·021	0·55	±1·70	−1·133	—	−0·376	−0·672
290	0·0535	1·38	±1·70	−1·143	−1·177	−0·380	−0·579
290	0·085	2·20	±1·70	−1·162	−0·986	−0·398	−0·580
290	0·1145	2·97	±1·70	−1·152	−1·090	−0·437	−0·639
60-deg swept-back wing: axis of oscillation at 0·288$\bar{c}$							
201	0	0	±1·69	−1·209	—	−0·055	—
201	0·0305	0·55	±1·69	−1·209	−0·759	−0·057	−0·408
201	0·0765	1·38	±1·69	−1·227	−0·849	−0·058	−0·397
201	0·122	2·20	±1·69	−1·246	−0·800	−0·059	−0·354
201	0·165	2·97	±1·69	−1·274	−0·733	−0·078	−0·349
290	0	0	±1·69	−1·232	—	−0·056	—
290	0·021	0·55	±1·69	−1·209	−0·835	−0·057	−0·309
290	0·0535	1·38	±1·69	−1·255	−0·863	−0·061	−0·347
290	0·085	2·20	±1·69	−1·255	−0·836	−0·064	−0·385
290	0·1145	2·97	±1·69	−1·292	−0·799	−0·080	−0·348

TABLE 3

$m_{\dot{\theta}}$: Free-Oscillation Results: 5·485-ft Span 90-deg Delta Wing

V (ft/sec)	α_{mean} (deg)	ω	T (sec)	I (slugs ft^2)	$m_{\dot{\theta}}$ Amp. = $\pm \frac{1}{2}$ deg	$m_{\dot{\theta}}$ Amp. = $\pm$ 1 deg	$m_{\dot{\theta}}$ Amp. = $\pm 1\frac{1}{2}$ deg	$m_{\dot{\theta}}$ Amp. = $\pm$ 2 deg
Axis of oscillation at 0·055$\bar{c}$ with body								
101	0	0·024	4·76	1117·4	−0·684	−0·678	−0·666	−0·666
101	0	0·038	2·97	462·9	−0·690	−0·695	−0·671	−0·676
101	0	0·0745	1·53	127·3	−0·692	−0·687	−0·671	−0·653
101	0	0·073	1·55	1175·6		−0·701		
101	0	0·163	0·696	129·1	−0·697	−0·695	−0·682	−0·684
101	0	0·221	0·514	129·1	−0·743	−0·727	−0·718	−0·728
101	0	0·2635	0·431	129·2	−0·725	−0·710	−0·711	−0·725
101	0	0·303	0·375	130·9	−0·743	−0·717	−0·753	−0·766
201	0	0·013	4·32	1117·4	−0·650	−0·637	−0·614	−0·614
201	0	0·0135	4·26	1128·6	−0·661	−0·638	−0·627	−0·627
201	0	0·0215	2·64	462·9	−0·654	−0·666	−0·647	−0·645
201	0	0·0420	1·36	127·3	−0·678	−0·687	−0·669	−0·658
201	0	0·0370	1·54	1175·6		−0·689		
201	0	0·0735	0·674	129·1	−0·649	−0·675	−0·669	−0·668
201	0	0·113	0·504	129·1	−0·676	−0·684	−0·676	−0·669
201	0	0·132	0·430	129·2	−0·682	−0·680	−0·675	−0·681
201	0	0·152	0·374	130·9	−0·699	−0·683	−0·684	−0·691
290	0	0·011	3·65	1117·4	−0·694	−0·691	−0·667	−0·667
290	0	0·0105	3·67	1128·6	−0·668	−0·668	−0·657	−0·657
290	0	0·017	2·32	462·9	−0·672	−0·650	−0·637	−0·635
290	0	0·033	1·19	127·3	−0·677	−0·679	−0·664	−0·658
290	0	0·026	1·51	1175·6		−0·695		
290	0	0·061	0·644	129·1	−0·692	−0·680	−0·675	−0·669
290	0	0·079	0·500	129·1	−0·673	−0·687	−0·686	−0·673
290	0	0·095	0·407	129·2	−0·691	−0·691	−0·690	−0·691
290	0	0·1065	0·370	130·9	−0·686	−0·683	−0·683	−0·683
Axis of oscillation at 0·328$\bar{c}$ with body								
101	0	0·022	5·110	798·6	−0·361	−0·341	−0·337	−0·303
101	0	0·0355	3·180	330·9	−0·373	−0·330	−0·324	−0·284
101	0	0·070	1·620	90·15	−0·333	−0·319	−0·327	−0·309
101	0	0·163	0·697	92·3	−0·348	−0·309	−0·322	−0·315
101	0	0·218	0·521	92·2	−0·336	−0·310	−0·302	−0·303
101	0	0·261	0·435	93·7	−0·307	−0·350	−0·324	−0·324
101	0							
201	0	0·011	5·165	798·6	−0·418	−0·394	−0·356	−0·349
201	0	0·0175	3·224	330·9	−0·277	−0·286	−0·269	−0·262
201	0	0·035	1·625	90·15	−0·340	−0·306	−0·307	−0·313
201	0	0·0815	0·698	92·3	−0·311	−0·324	−0·308	−0·305
201	0	0·109	0·522	92·2	−0·309	−0·307	−0·309	−0·312
201	0	0·1305	0·435	93·7	−0·309	−0·310	−0·298	−0·309
201	0	0·1465	0·387	95·7	−0·329	−0·333	−0·303	−0·302
290	0	0·0075	5·280	798·6	−0·394	−0·339	−0·357	−0·331
290	0	0·012	3·280	330·9	−0·351	−0·366	−0·358	−0·314
290	0	0·0235	1·660	90·15	−0·330	−0·332	−0·347	−0·335
290	0	0·056	0·706	92·3	−0·338	−0·319	−0·318	−0·304
290	0	0·075	0·524	92·2	−0·331	−0·314	−0·321	−0·317
290	0	0·0905	0·435	93·7	−0·319	−0·325	−0·315	−0·302
290	0	0·102	0·387	95·7	−0·309	−0·337	−0·312	−0·321

TABLE 3—*continued*

$m_{\dot{\theta}}$: Free-Oscillation Results: 5·485-ft. Span 90-deg Delta Wing

V (ft/sec)	α_{mean} (deg)	ω	T (sec)	I (slugs ft²)	$m_{\dot{\theta}}$ Amp. = $\pm \frac{1}{2}$ deg	$m_{\dot{\theta}}$ Amp. = ± 1 deg	$m_{\dot{\theta}}$ Amp. = $\pm 1\frac{1}{2}$ deg	$m_{\dot{\theta}}$ Amp. = ± 2 deg
Axis of oscillation at $0 \cdot 328\bar{c}$: wing alone								
101	0	0·0225	5·068	794·9	−0·389	−0·330	−0·344	−0·309
101	0	0·036	3·172	326·8	−0·354	−0·325	−0·343	−0·314
101	0	0·0715	1·592	88·92	−0·323	−0·327	−0·325	−0·318
201	0	0·011	5·110	794·9	−0·390	−0·388	−0·350	−0·327
201	0	0·018	3·172	326·8	−0·303	−0·280	−0·300	−0·280
201	0	0·0355	1·593	88·92	−0·291	−0·316	−0·321	−0·317
290	0	0·0075	5·10	794·9	−0·374	−0·390	−0·340	−0·345
290	0	0·0125	3·18	326·8	−0·380	−0·315	−0·331	−0·336
290	0	0·0245	1·593	88·92	−0·303	−0·327	−0·343	−0·324
					$m_{\dot{\theta}}$ Amp. = $\pm \frac{1}{2}$ deg	$m_{\dot{\theta}}$ Amp. = ± 1 deg	$m_{\dot{\theta}}$ Amp. = ± 2 deg	$m_{\dot{\theta}}$ Amp. = ± 3 deg
101	0	0·071	1·60	51·61	−0·326	−0·310	−0·322	−0·305
201	0	0·0355	1·605	51·61	−0·322	−0·320	−0·314	−0·304
101	5·0	0·071	1·60	51·59	−0·342	−0·350	−0·341	−0·332
201	5·0	0·0355	1·60	51·59	−0·300	−0·313	−0·327	−0·330
101	7·1	0·071	1·60	50·46	−0·268	−0·325	−0·312	−0·328
201	7·1	0·0355	1·60	50·46	−0·303	−0·282	−0·301	−0·294
101	8·35	0·071	1·59	50·39	−0·309	−0·347	−0·350	−0·369
201	8·35	0·036	1·58	50·39	−0·308	−0·284	−0·298	−0·307
101	10·55	0·071	1·60	50·51	−0·486	−0·471	−0·493	−0·496
201	10·55	0·0355	1·60	50·51	−0·377	−0·363	−0·425	−0·509
101	12·25	0·071	1·61	49·83	−0·555	−0·634	−0·631	−0·630
201	12·25	0·0355	1·60	49·83	−0·625	−0·702	−0·740	−0·712
101	14·80	0·071	1·60	47·61	−0·639	−0·913	−0·793	−0·790
201	14·80	0·0355	1·60	47·61	−0·566	−0·313	−0·651	−0·592

TABLE 4

$m_{\dot{\theta}}$: Free-Oscillation Results: 3·35-ft Span 90-deg Delta Wing (Without Body)

V (ft/sec)	ω	T (sec)	I (slugs ft²)	$m_{\dot{\theta}}$ Amp. = ± 1 deg	$m_{\dot{\theta}}$ Amp. = ± 2 deg
Axis of oscillation at $0{\cdot}055\bar{c}$ $\alpha_{mean} = 0$ deg					
101	0·0145	4·85	593·0	−0·718	−0·721
101	0·023	3·03	248·4	−0·740	−0·718
101	0·0475	1·47	65·1	−0·763	−0·714
101	0·104	0·672	66·1	−0·778	−0·721
101	0·139	0·502	66·0	−0·739	−0·718
101	0·166	0·421	66·4	−0·745	−0·749
201	0·008	4·58	593·0	−0·022	−0·848
201	0·0125	2·36	248·4	−0·747	−0·718
201	0·0255	1·43	65·1	−0·721	−0·751
201	0·054	0·665	66·1	−0·732	−0·700
201	0·0725	0·496	66·0	−0·723	−0·700
201	0·086	0·419	66·4	−0·737	−0·722
290	0·005	4·26	593·0	−0·954	−0·895
290	0·009	2·67	248·4	−0·767	−0·740
290	0·018	1·33	65·1	−0·732	−0·750
290	0·037	0·654	66·1	−0·754	−0·753
290	0·049	0·496	66·0	−0·753	−0·699
290	0·0585	0·415	66·4	−0·739	−0·739
Axis of oscillation at $0{\cdot}328\bar{c}$ $\alpha_{mean} = 0$ deg					
101	0·014	4·94	461·2	−0·371	−0·335
101	0·0225	3·08	191·5	−0·362	−0·372
101	0·046	1·52	50·6	−0·372	−0·371
101	0·103	0·679	52·6	−0·339	−0·415
101	0·165	0·424	53·6	−0·358	−0·384
201	0·007	5·00	461·2	−0·330	−0·380
201	0·0115	3·09	191·5	−0·401	−0·335
201	0·0225	1·54	50·6	−0·361	−0·339
201	0·0515	0·680	52·6	−0·359	−0·373
201	0·0825	0·424	53·6	−0·368	−0·377
290	0·005	5·01	461·2	−0·437	−0·406
290	0·003	3·10	191·5	−0·394	−0·437
290	0·0155	1·55	50·6	−0·370	−0·391
290	0·036	0·678	52·6	−0·350	−0·365
290	0·057	0·424	53·6	−0·361	−0·377

TABLE 5

$m_{\dot{\theta}}$: Free-Oscillation Results: 60-deg Swept-back Wing (With Body)

V (ft/sec)	ω	T (sec)	I (slugs ft^2)	$m_{\dot{\theta}}$ Amp. = $\pm \frac{1}{2}$ deg	$m_{\dot{\theta}}$ Amp. = ± 1 deg	$m_{\dot{\theta}}$ Amp. = $\pm 1\frac{1}{2}$ deg	$m_{\dot{\theta}}$ Amp. = ± 2 deg
Axis of oscillation at $0 \cdot 0\bar{c}$: $\alpha_{mean} = 0$ deg							
101	0·0235	4·743	1079·1	—0·659	—0·674	—0·627	—0·681
101	0·029	3·846	726·8	—0·704	—0·710	—0·714	—0·699
101	0·037	3·155	457·5	—0·664	—0·721	—0·695	—0·669
101	0·049	2·26	268·3	—0·732	—0·724	—0·702	—0·699
101	0·0715	1·550	127·2	—0·698	—0·725	—0·687	—0·688
101	0·1585	0·700	128·5	—0·687	—0·726	—0·694	—0·727
101	0·212	0·523	130·4	—0·730	—0·725	—0·740	—0·729
201	0·013	4·250	1079·1	—0·663	—0·598	—0·638	—0·609
201	0·016	3·424	726·8	—0·612	—0·622	—0·623	—0·661
201	0·021	2·676	457·5	—0·625	—0·630	—0·612	—0·613
201	0·0275	2·014	268·3	—0·643	—0·634	—0·643	—0·643
201	0·040	1·385	127·2	—0·659	—0·635	—0·629	—0·617
201	0·081	0·686	128·5	—0·673	—0·647	—0·644	—0·647
201	0·108	0·514	130·4	—0·671	—0·672	—0·680	—0·644
201	0·145	0·383	133·6	—0·708	—0·703	—0·689	—0·655
290	0·0105	3·684	1079·1	—0·629	—0·577	—0·559	—0·551
290	0·013	2·972	726·8	—0·622	—0·588	—0·564	—0·613
290	0·0165	2·342	457·5	—0·639	—0·636	—0·600	—0·641
290	0·022	1·768	268·3	—0·602	—0·597	—0·606	—0·585
290	0·0315	1·218	127·2	—0·641	—0·635	—0·614	—0·632
290	0·0585	0·660	128·5	—0·634	—0·632	—0·611	—0·656
290	0·077	0·502	130·4	—0·650	—0·654	—0·633	—0·630
290	0·105	0·372	133·6	—0·682	—0·670	—0·680	—0·640
Axis of oscillation at $0 \cdot 288\bar{c}$: $\alpha_{mean} = 0$ deg							
101	0·022	5·000	980·0	—0·360	—0·338	—0·349	—0·354
101	0·0355	3·128	407·4	—0·350	—0·332	—0·339	—0·337
101	0·068	1·634	115·1	—0·348	—0·349	—0·363	—0·353
101	0·069	1·605	115·3	—0·328	—0·334	—0·373	—0·364
101	0·905	1·224	117·1	—0·364	—0·351	—0·343	—0·343
101	0·215	0·522	117·7	—0·386	—0·311	—0·340	—0·356
201	0·0115	4·884	980	—0·275	—0·300	—0·323	—0·339
201	0·018	3·064	407·4	—	—0·330	—0·310	—0·306
201	0·025	2·22	164·8	—	—0·281	—	—
201	0·035	1·585	115·1	—0·317	—0·329	—0·316	—0·318
201	0·0355	1·56	115·3	—0·340	—0·335	—0·334	—0·332
201	0·046	1·206	117·1	—0·327	—0·338	—0·323	—0·330
201	0·107	0·519	117·7	—0·353	—0·348	—0·340	—0·356
201	0·141	0·394	118·7	—0·337	—0·338	—0·327	—
290	0·082	4·698	980	—0·361	—0·329	—0·317	—0·328
290	0·013	2·938	407·4	—0·291	—0·307	—0·302	—0·299
290	0·0195	1·96	181·7	—	—0·336	—	—
290	0·025	1·546	115·1	—0·264	—0·276	—0·292	—0·287
290	0·0255	1·528	113·3	—	—0·273	—	—
290	0·255	1·525	115·3	—0·273	—0·283	—0·287	—0·292
290	0·0325	1·182	117·1	—0·331	—0·330	—0·320	—0·310
290	0·075	0·516	117·7	—0·329	—0·327	—0·318	—0·328
290	0·098	0·393	118·7	—0·349	—0·339	—0·336	—

TABLE 6

$m_{\dot\theta}$: Free-Oscillation Results: 40-deg Swept-back Wing (With Body)

V (ft/sec)	ω	T (sec)	I (slugs ft^2)	$m_{\dot\theta}$ Amp. = $\pm \frac{1}{2}$ deg	$m_{\dot\theta}$ Amp. = $\pm$ 1 deg	$m_{\dot\theta}$ Amp. = $\pm 1\frac{1}{2}$ deg	$m_{\dot\theta}$ Amp. = $\pm$ 2 deg
Axis of oscillation at $-0\cdot051\bar{c}$: $\alpha_{\text{mean}} = 0$ deg							
101	0·0235	4·50	1104·0	−0·712	−0·742	−0·719	−0·685
101	0·0235	4·48	1103·6	−0·721	−0·714	−0·714	−0·714
101	0·0375	2·82	467·0	−0·776	−0·750	−0·750	−0·750
101	0·0725	1·47	132·4	−0·775	−0·771	−0·750	−0·728
101	0·153	0·695	134·6	−0·799	−0·803	−0·804	−0·791
101	0·204	0·52	133·7	−0·877	−0·815	−0·809	−0·754
201	0·0145	3·68	1104·0	−0·688	−0·690	−0·734	−0·663
201	0·0145	3·68	1103·6	—	−0·685	−0·685	−0·685
201	0·023	2·30	467·0	−0·737	−0·740	−0·741	−0·741
201	0·044	1·21	132·4	−0·767	−0·758	−0·747	−0·737
201	0·0795	0·667	134·6	−0·769	−0·758	−0·767	−0·754
201	0·103	0·518	133·7	−0·776	−0·753	−0·758	−0·733
201	0·125	0·425	135·5	−0·790	−0·765	−0·766	−0·741
290	0·012	3·00	1104·0	−0·787	−0·803	−0·797	−0·786
290	0·012	3·00	1103·6	−0·788	−0·775	−0·775	−0·775
290	0·0195	1·90	467·0	−0·776	−0·743	−0·745	−0·745
290	0·037	1·00	132·4	−0·759	−0·736	−0·730	−0·723
290	0·059	0·625	134·6	−0·733	−0·730	−0·715	−0·695
290	0·074	0·498	133·7	−0·725	−0·720	−0·681	−0·670
290	0·098	0·372	136·5	−0·728	−0·724	−0·715	−0·719
Axis of oscillation at $0\cdot258\bar{c}$: $\alpha_{\text{mean}} = 0$ deg							
101	0·022	4·84	872·5	−0·257	−0·361	−0·361	−0·361
101	0·0355	3·00	375·0	−0·319	−0·328	−0·344	−0·344
101	0·0685	1·564	102·5	−0·315	−0·325	−0·322	−0·309
101	0·0685	1·564	102·5	−0·349	−0·323	−0·322	−0·314
101	0·107	0·988	103·4	−0·339	−0·324	−0·375	−0·359
101	0·152	0·701	104·0	−0·350	−0·340	−0·328	−0·341
101	0·202	0·524	104·0	−0·354	−0·386	−0·372	−0·376
101	0·241	0·440	104·0	−0·416	−0·426	−0·376	−0·365
101	0·278	0·382	103·9	−0·396	−0·368	−0·347	−0·328
201	0·0115	4·58	812·5	−0·324	−0·322	−0·299	−0·299
201	0·0115	4·53	870·0	−0·320	−0·321	−0·302	−0·302
201	0·0185	2·85	375·0	−0·342	−0·368	−0·351	−0·351
201	0·0185	2·86	364·2	−0·368	−0·350	−0·365	−0·366
201	0·036	1·48	102·5	−0·297	−0·307	−0·308	−0·312
201	0·036	1·48	102·5	—	−0·313	—	—
201	0·054	0·984	103·4	−0·299	−0·334	−0·333	−0·322
201	0·0765	0·692	104·0	−0·324	−0·338	−0·316	−0·319
201	0·102	0·522	104·0	−0·320	−0·337	−0·334	−0·334
201	0·121	0·438	104·0	−0·352	−0·356	−0·351	−0·339
201	0·138	0·384	103·9	−0·344	−0·330	−0·316	−0·347
290	0·0085	4·22	872·5	−0·404	−0·405	−0·392	−0·392
290	0·0085	4·28	870·0	−0·428	−0·412	−0·403	−0·403
290	0·014	2·68	375·0	−0·340	−0·340	−0·351	−0·323
290	0·026	0·40	102·5	−0·291	−0·337	−0·330	−0·287
290	0·039	0·942	103·4	−0·304	−0·347	−0·341	−0·333
290	0·0535	0·684	104·0	−0·318	−0·318	−0·322	−0·311
290	0·071	0·518	104·0	−0·314	−0·331	−0·332	−0·317
290	0·0845	0·436	104·0	−0·327	−0·331	−0·321	−0·305
290	0·0955	0·384	103·9	−0·310	−0·323	−0·311	−0·293

TABLE 7

$m_{\dot{\theta}}$: Free-Oscillation Results: 40-deg Swept-back Wing (Without Body)

V (ft/sec)	ω	T (sec)	I (slugs ft^2)	$m_{\dot{\theta}}$ Amp. $= \pm 1$ deg	$m_{\dot{\theta}}$ Amp. $= \pm 2$ deg
Axis of oscillation at $-0\cdot051\bar{c}$ $\alpha_{mean} = 0$ deg					
101	0·027	4·23	861·9	−0·568	−0·570
101	0·043	2·67	360·1	−0·606	−0·640
101	0·0835	1·37	97·7	−0·616	−0·612
101	0·1665	0·689	102·3	−0·655	−0·640
201	0·018	3·22	861·9	−0·545	−0·565
201	0·028	2·05	360·1	−0·540	−0·558
201	0·054	1·06	97·7	−0·539	−0·585
201	0·091	0·634	102·3	−0·583	−0·604
201	0·1415	0·405	103·3	−0·625	−0·634
290	0·016	2·52	861·9	−0·511	−0·539
290	0·0245	1·61	360·1	−0·491	−0·529
290	0·048	0·835	97·7	−0·494	−0·521
290	0·069	0·576	102·3	−0·546	−0·568
290	0·0995	0·400	103·3	−0·549	−0·574
Axis of oscillation at $0\cdot258\bar{c}$ $\alpha_{mean} = 0$ deg					
101	0·024	4·77	804·0	−0·278	−0·303
101	0·0385	2·99	332·8	−0·306	−0·316
101	0·0765	1·50	91·2	−0·305	−0·295
101	0·0765	1·50	63·8	−0·308	−0·311
101	0·167	0·689	91·7	−0·319	−0·321
101	0·268	0·429	92·7	−0·348	−0·363
201	0·013	4·38	804·0	−0·249	−0·287
201	0·021	2·74	332·8	−0·282	−0·317
201	0·0415	1·39	91·2	−0·313	−0·309
201	0·0425	1·35	63·8	−0·308	−0·315
201	0·085	0·675	91·7	−0·293	−0·313
201	0·135	0·426	92·7	−0·316	−0·326
290	0·010	3·94	804·0	−0·190	−0·258
290	0·016	2·47	332·8	−0·316	−0·330
290	0·0315	1·26	91·2	−0·304	−0·318
290	0·033	1·20	63·8	−0·290	−0·300
290	0·061	0·653	91·7	−0·280	−0·304
290	0·0945	0·422	92·7	−0·282	−0·303
Axis of oscillation at $0\cdot572\bar{c}$ $\alpha_{mean} = 0$ deg					
101	0·0535	2·14	559·1	−0·411	−0·429
101	0·084	1·37	234·0	−0·394	−0·387
101	0·1615	0·713	64·6	−0·376	−0·377
101	0·227	0·506	65·0	−0·293	−0·407
201	0·024	2·38	559·1	−0·465	−0·465
201	0·0375	1·53	234·0	−0·457	−0·468
201	0·0715	0·804	64·6	−0·442	−0·446
201	0·107	0·536	65·0	−0·445	−0·461
290	0·0125	3·22	559·1	−0·669	−0·764
290	0·0195	2·06	234·0	−0·570	−0·691
290	0·038	1·06	64·6	−0·522	−0·604
290	0·0675	0·590	65·0	−0·581	−0·603

TABLE 8

Values of z_w Obtained by Method of Free Oscillations: 5·485-ft Span 90-deg Delta Wing (α_{mean} = 0 deg)

V (ft/sec)	ω	f (c.p.s.)	Amplitude (per cent $\bar{c}$)	z_w Wing alone	z_w With body
101	0·0499	0·437	±4·56	—	−1·476
101	0·0505	0·442	±4·56	−1·478	—
101	0·101	0·887	±4·56	—	−1·489
101	0·105	0·917	±4·56	−1·475	—
101	0·119	1·040	±4·56	−1·486	—
101	0·130	1·135	±4·56	—	−1·450
101	0·162	1·422	±4·56	—	−1·485
101	0·170	1·488	±4·56	−1·456	—
101	0·182	1·595	±4·56	—	−1·478
201	0·0250	0·437	±4·56	—	−1·506
201	0·0252	0·442	±4·56	−1·489	—
201	0·0506	0·887	±4·56	—	−1·529
201	0·0524	0·917	±4·56	−1·486	—
201	0·0594	1·040	±4·56	−1·506	—
201	0·0648	1·135	±4·56	—	−1·501
201	0·0812	1·422	±4·56	—	−1·565
201	0·0850	1·488	±4·56	−1·519	—
201	0·0911	1·595	±4·56	—	−1·550
101	0·0499	0·437	±9·12	—	−1·457
101	0·0505	0·442	±9·12	−1·442	—
101	0·101	0·887	±9·12	—	−1·466
101	0·105	0·917	±9·12	−1·443	—
101	0·119	1·040	±9·12	−1·446	—
101	0·130	1·135	±9·12	—	−1·472
101	0·162	1·422	±9·12	—	−1·462
101	0·170	1·488	±9·12	−1·479	—
101	0·182	1·595	±9·12	—	−1·515
201	0·0250	0·437	±9·12	—	−1·491
201	0·0252	0·442	±9·12	−1·490	—
201	0·0506	0·887	±9·12	—	−1·524
201	0·0524	0·917	±9·12	−1·496	—
201	0·0594	1·040	±9·12	−1·497	—
201	0·0648	1·135	±9·12	—	−1·558
201	0·0812	1·422	±9·12	—	−1·548
201	0·0850	1·488	±9·12	−1·535	—
201	0·0911	1·595	±9·12	—	−1·544

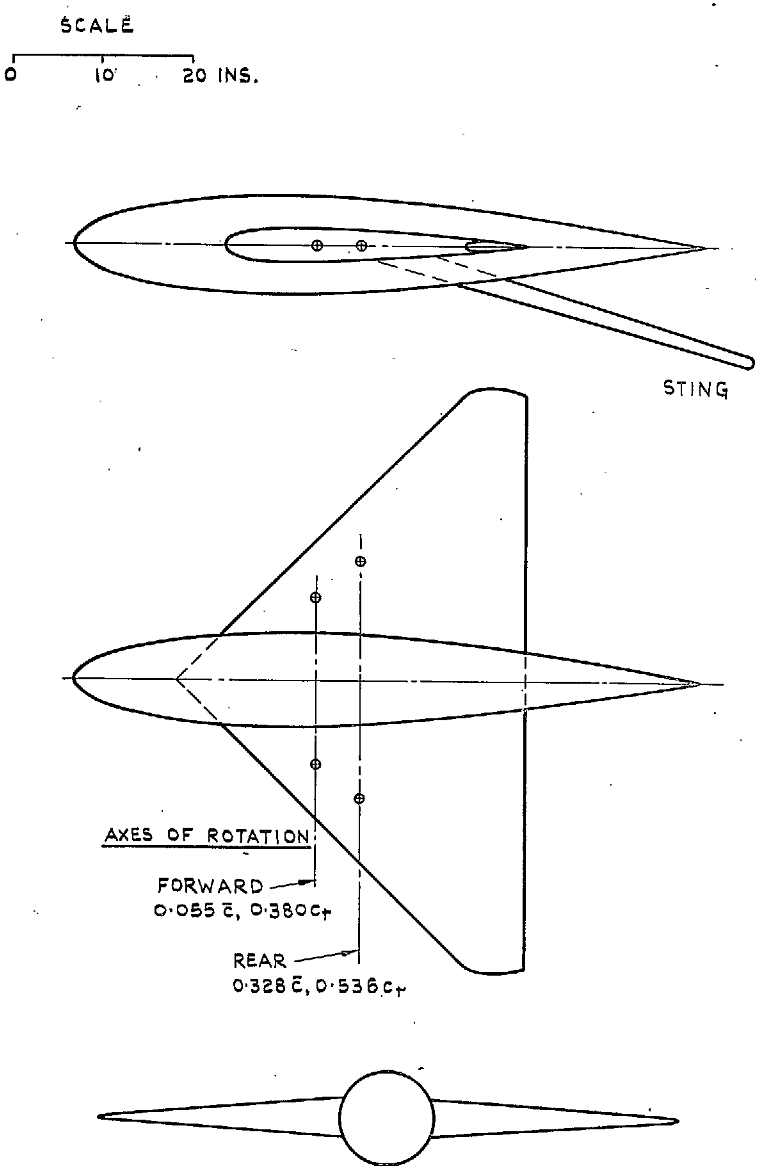

FIG. 1. 90-deg delta wing model.

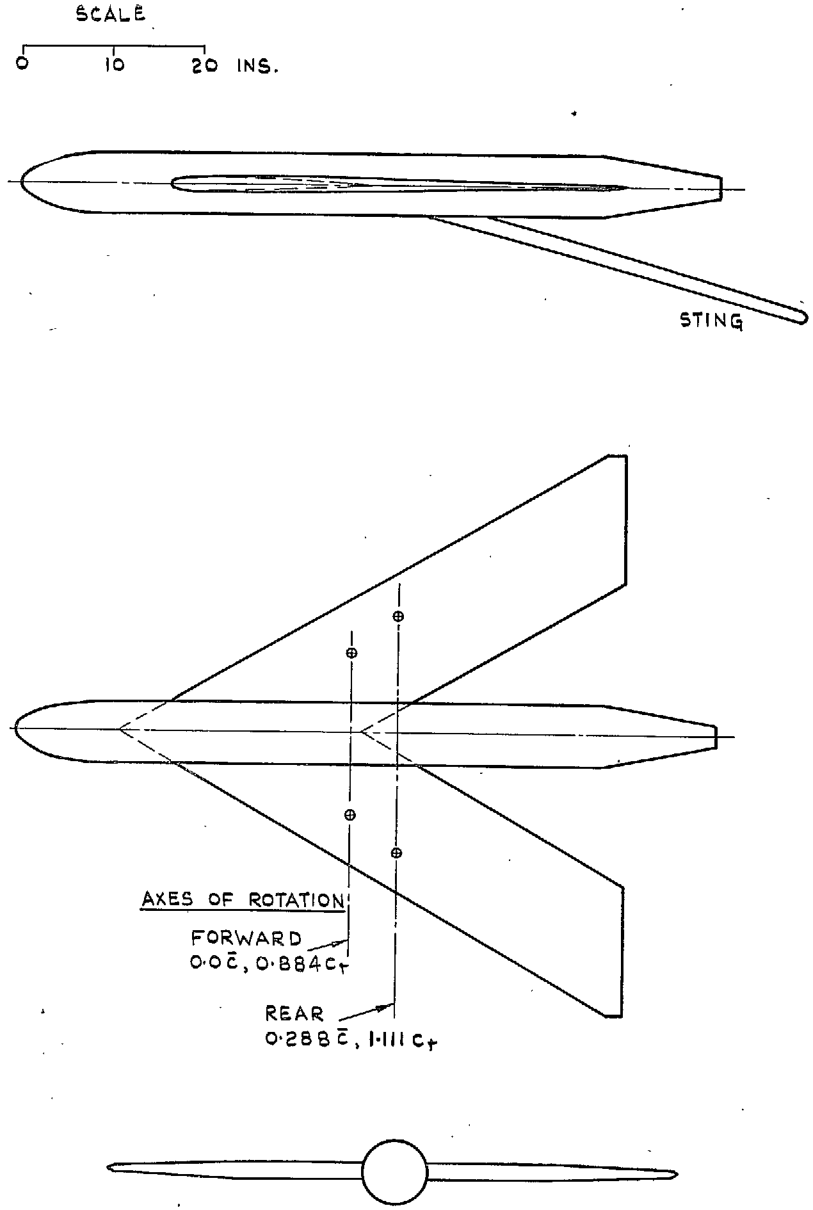

FIG. 2. 60-deg swept-back wing model.

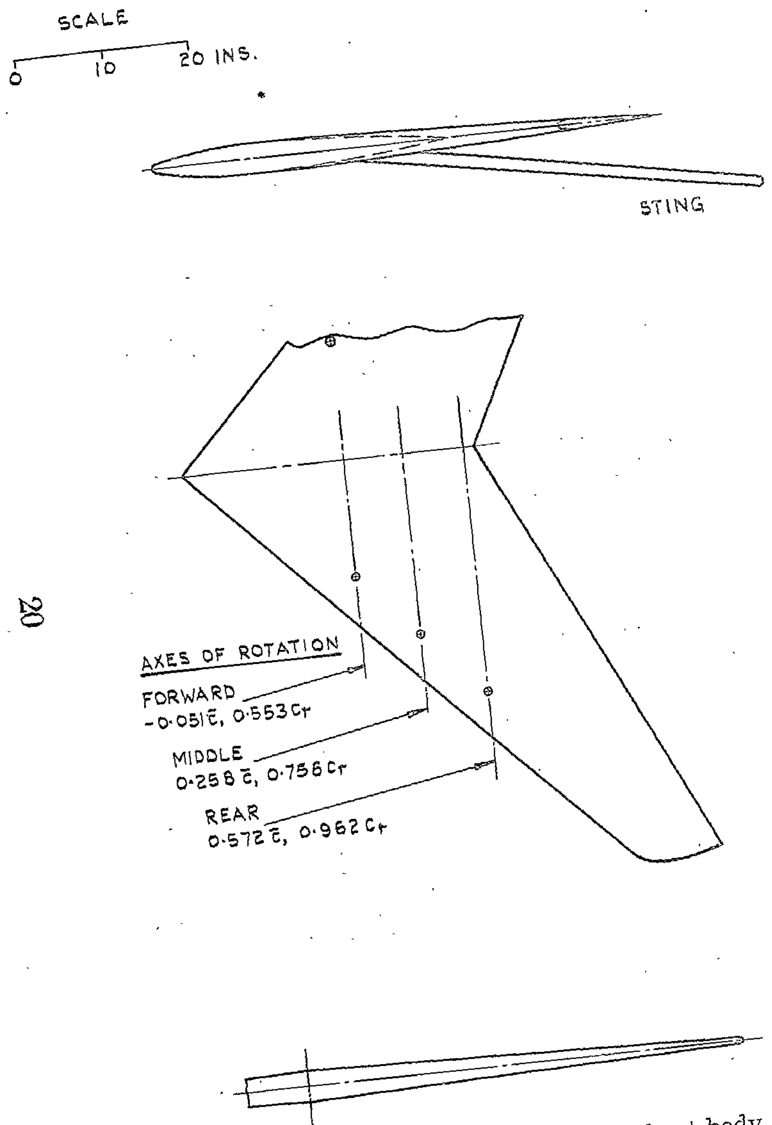

FIG. 3. 40-deg swept-back wing without body.

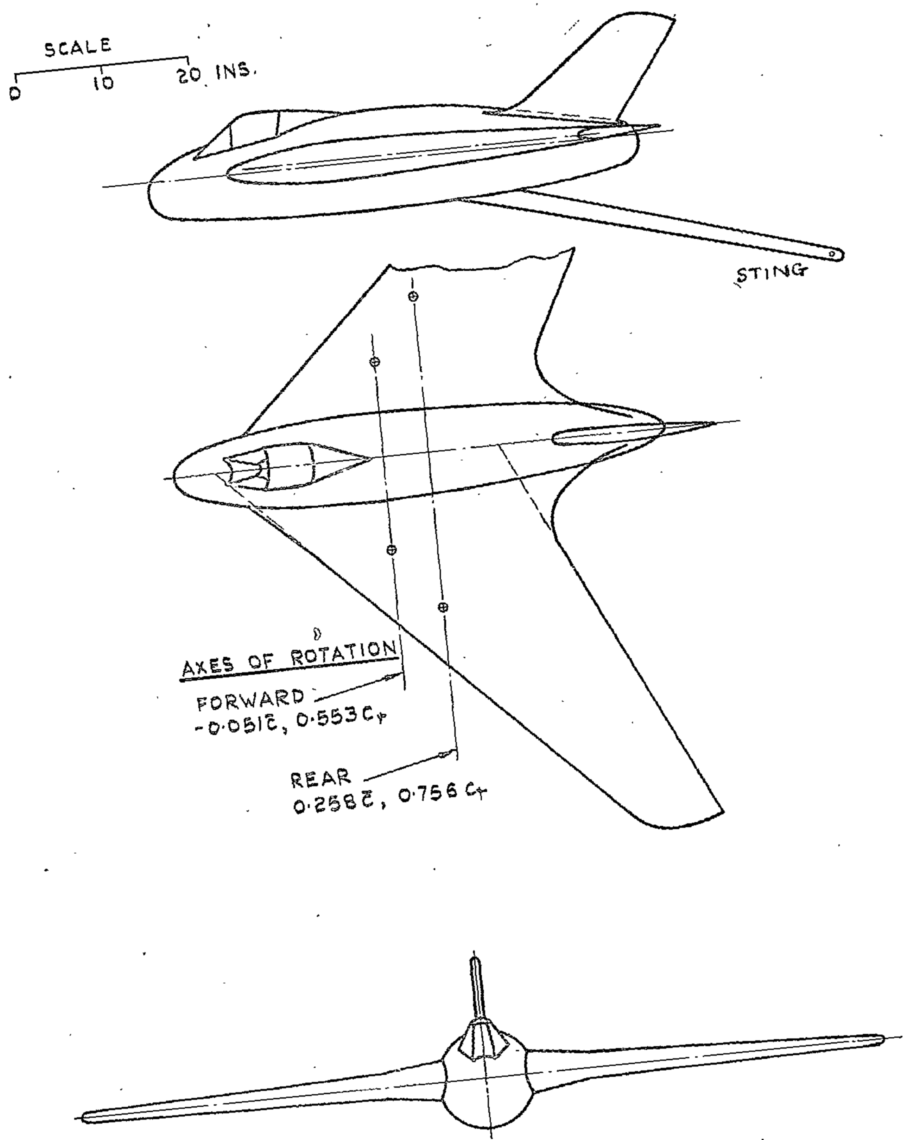

FIG. 4. 40-deg swept-back wing model with body.

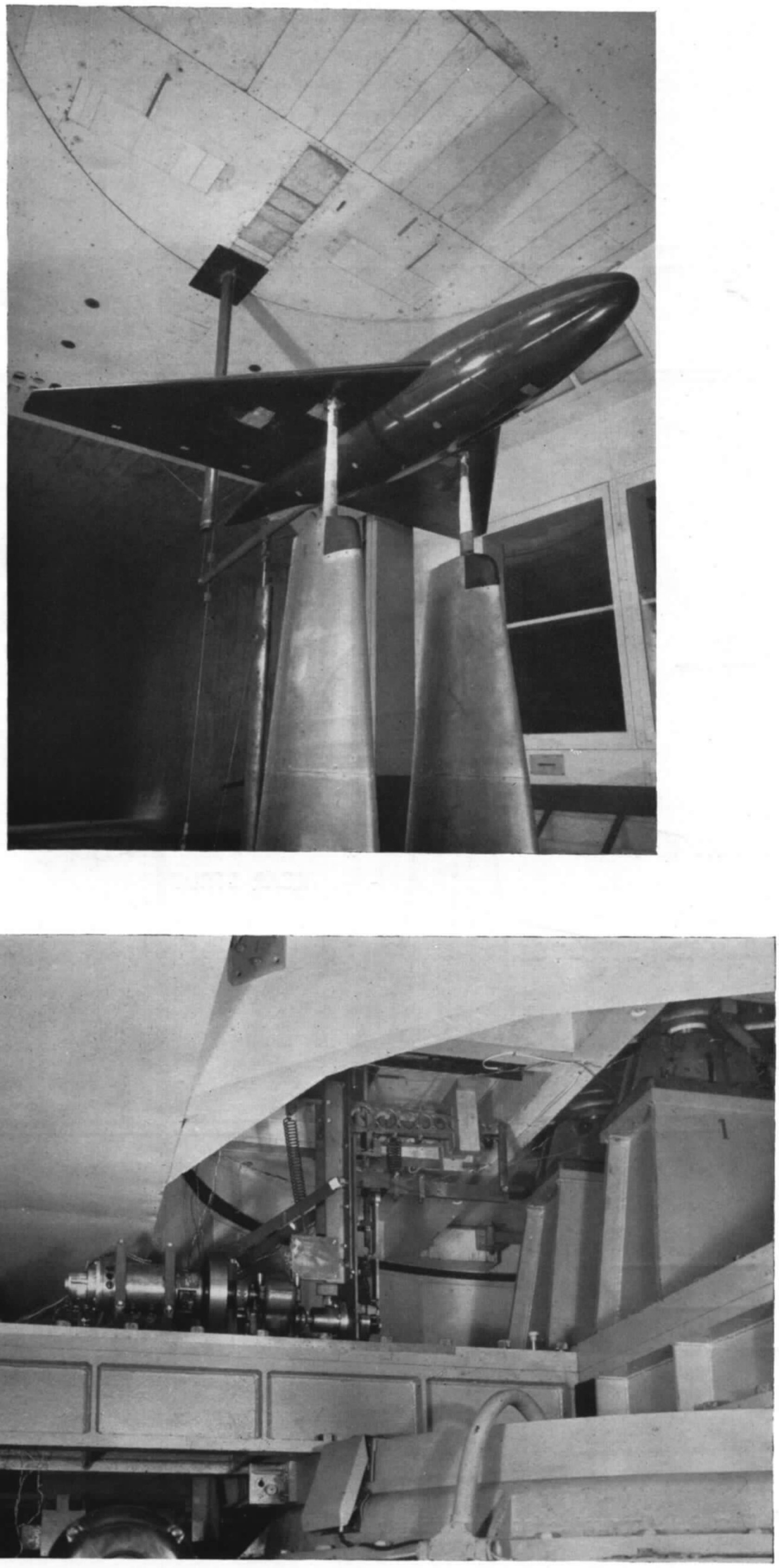

FIG. 5. Measurement of longitudinal derivatives by method of inexorable forcing.

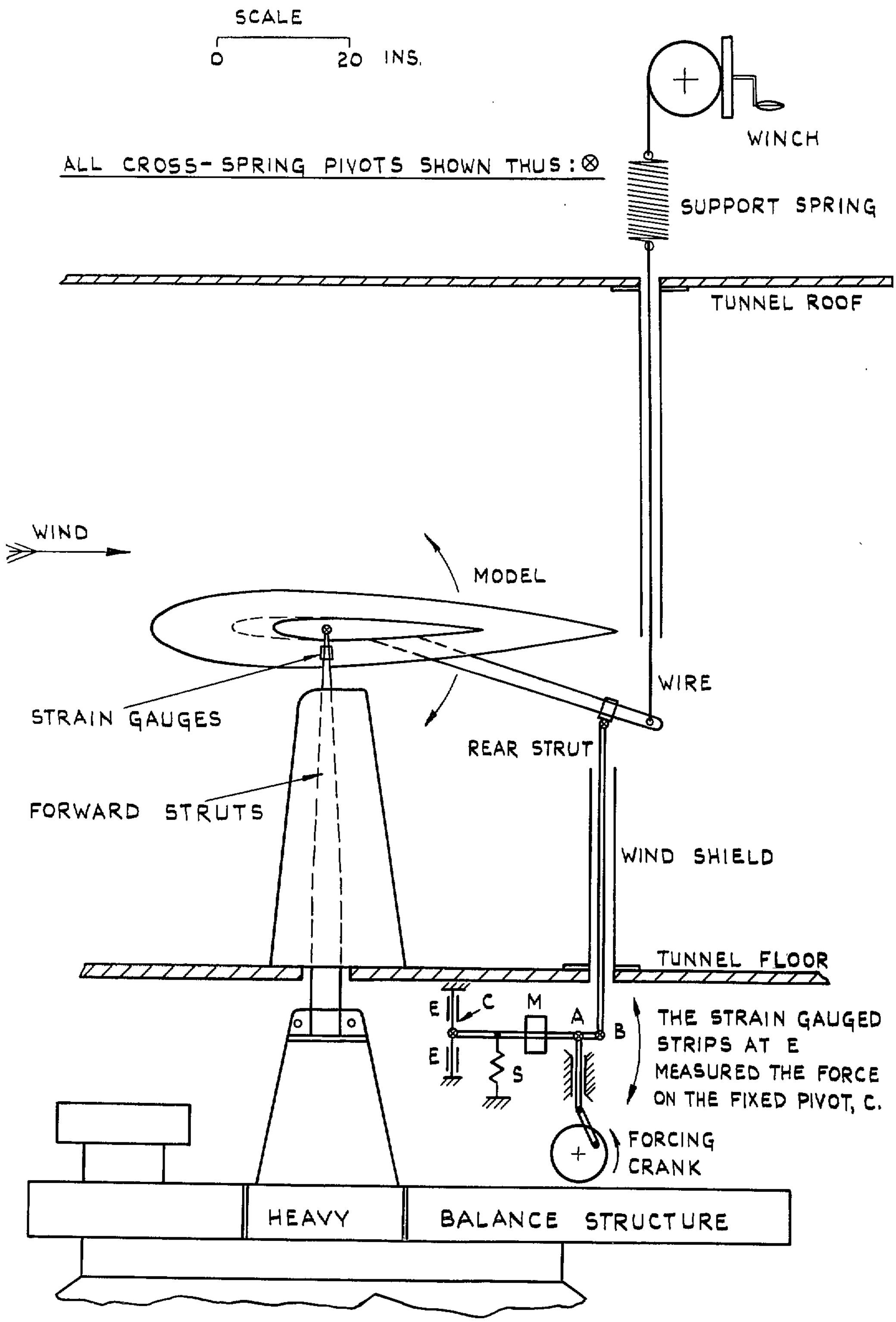

FIG. 6. Apparatus for measuring z_θ, $z_{\dot\theta}$, m_θ, $m_{\dot\theta}$ by method of inexorable forcing.

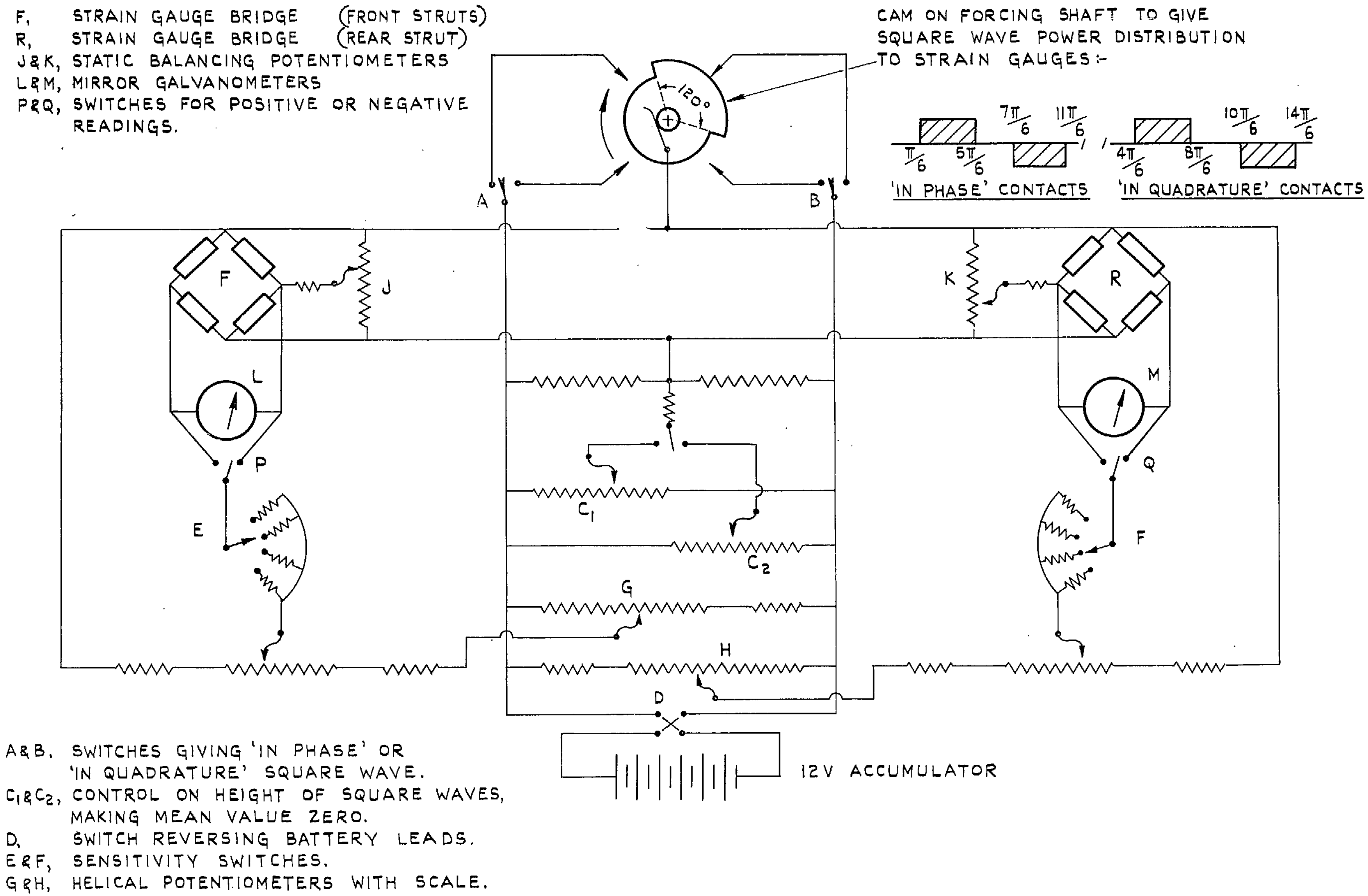

FIG. 7. Wiring diagram for inexorable forcing apparatus.

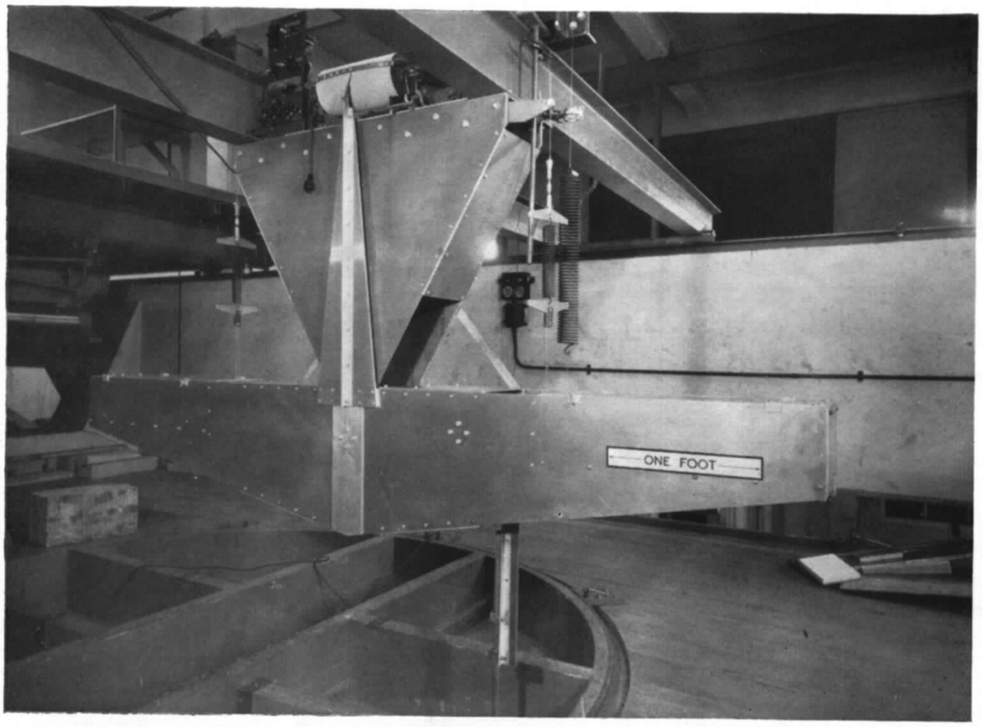

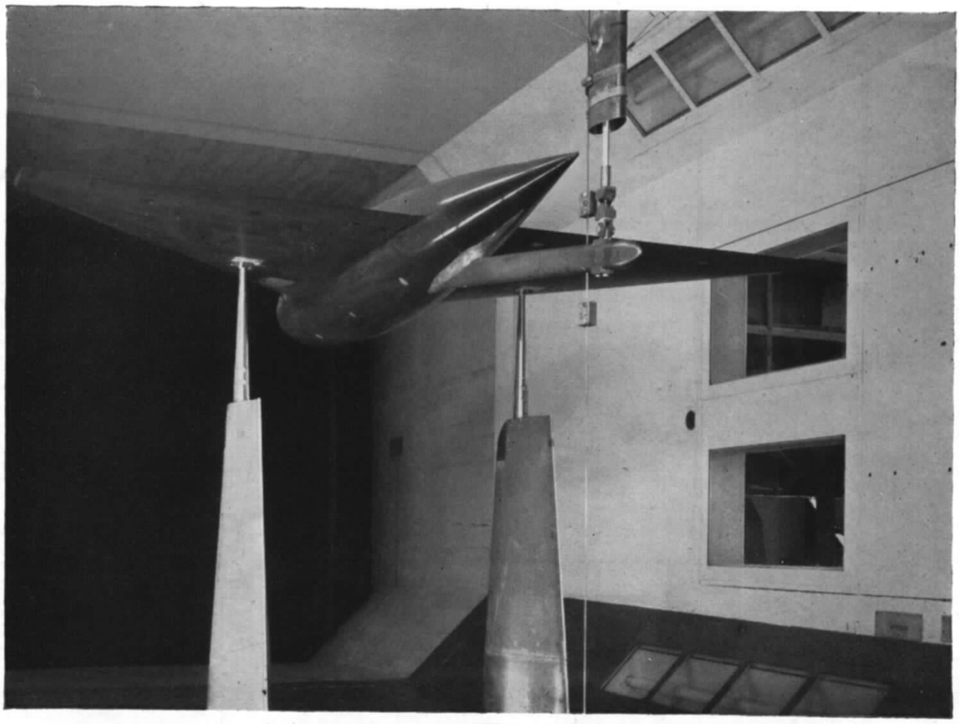

FIG. 8. Measurement of damping in pitch by method of free oscillations.

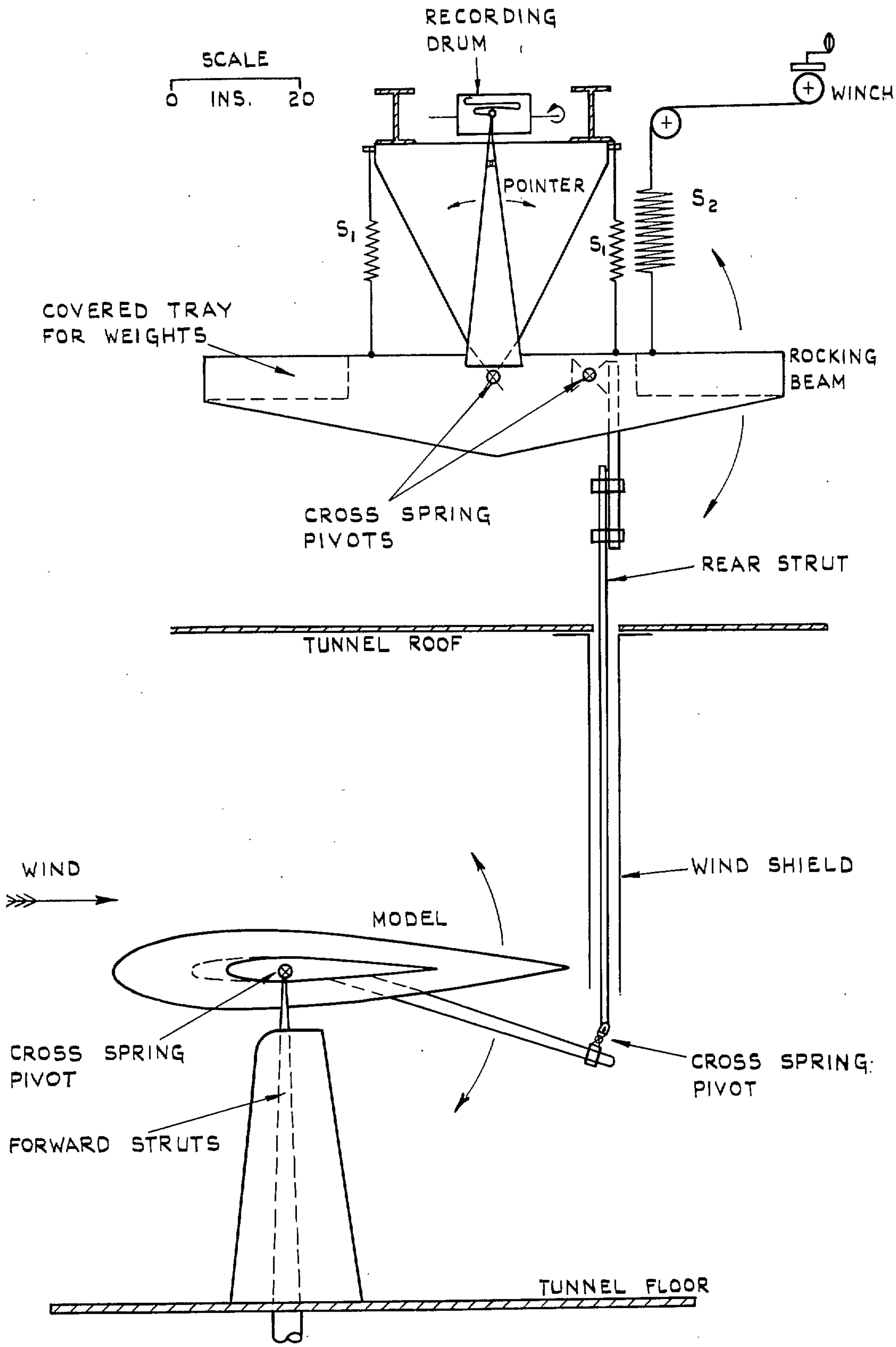

FIG. 9. Apparatus for measuring damping in pitch, $m_{\dot{\theta}}$, by method of free oscillations.

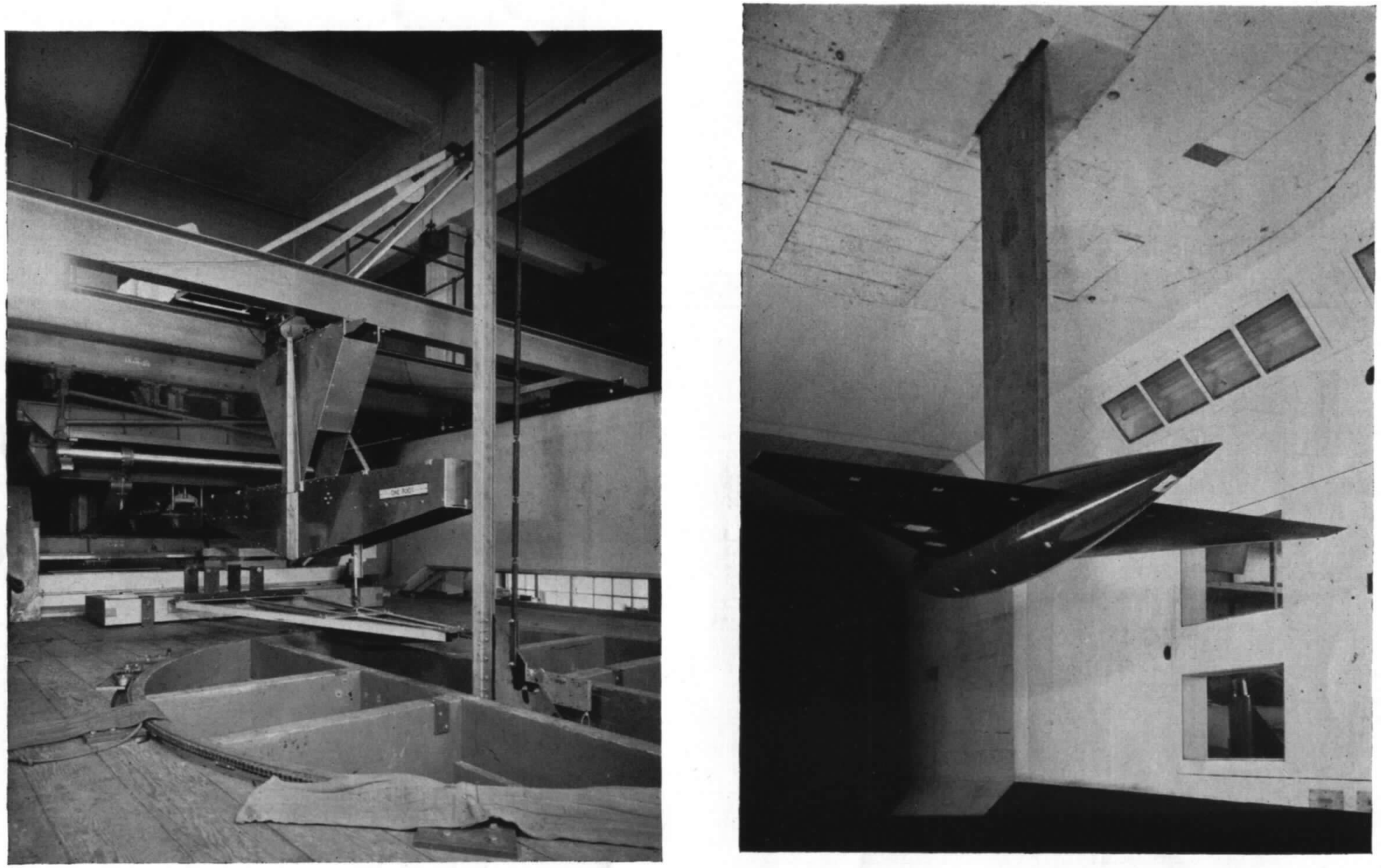

FIG. 10. Measurement of heaving-motion damping by method of free oscillations.

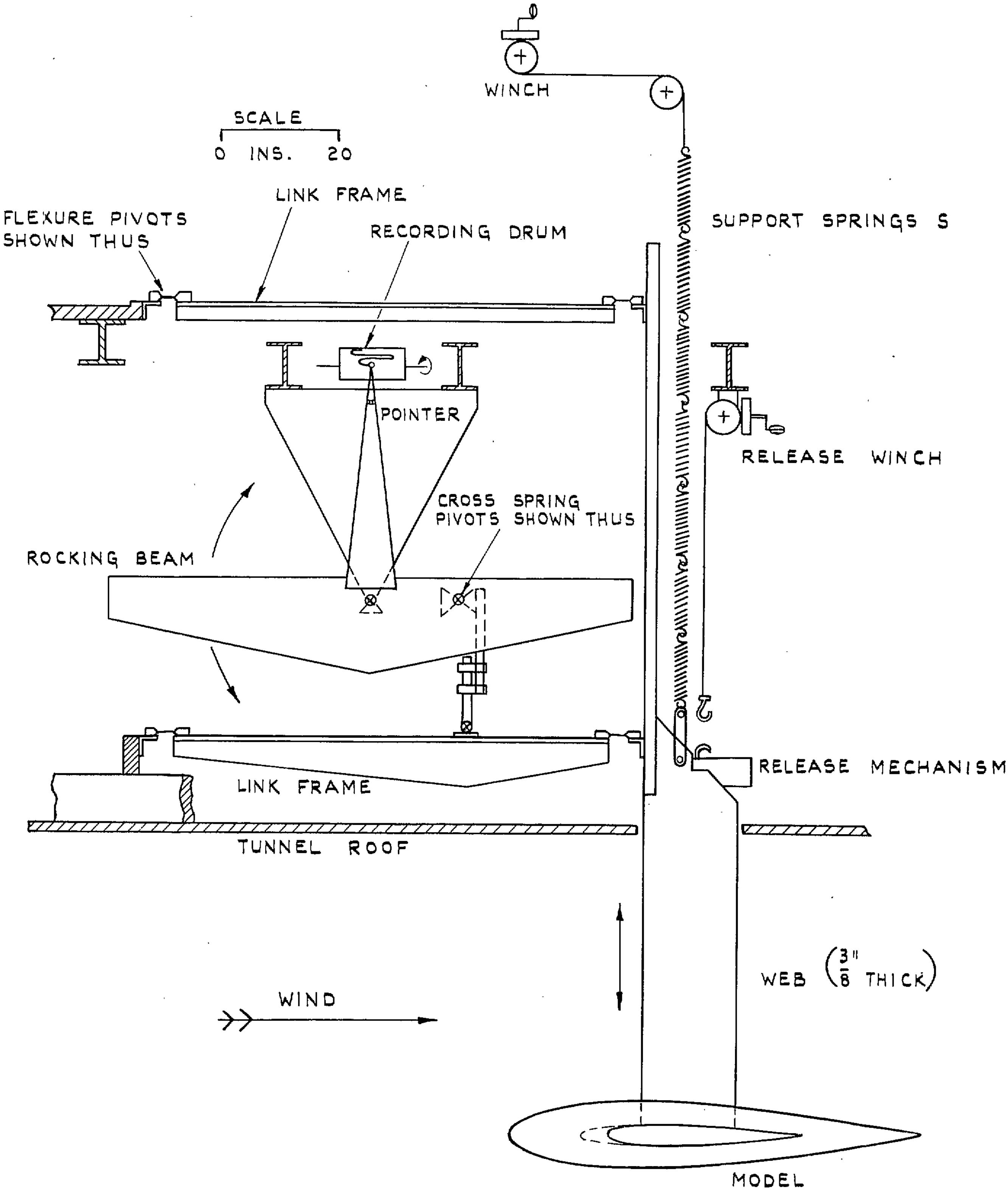

FIG. 11. Apparatus for measuring z_w by method of free oscillations.

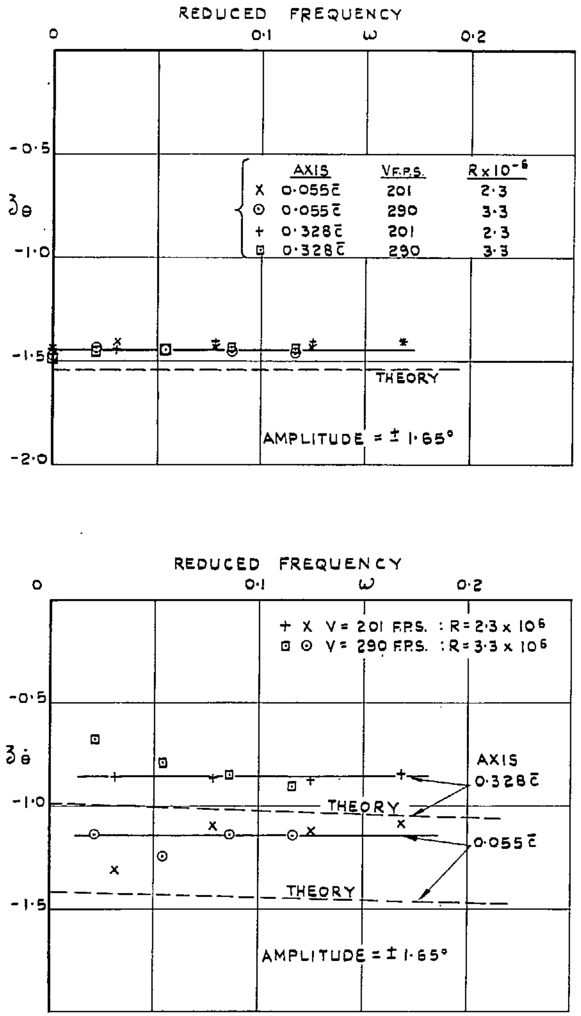

FIG. 12. Values of z_θ and $z_{\dot\theta}$. 5·485-ft span 90-deg delta wing with body. Method of inexorable forcing.

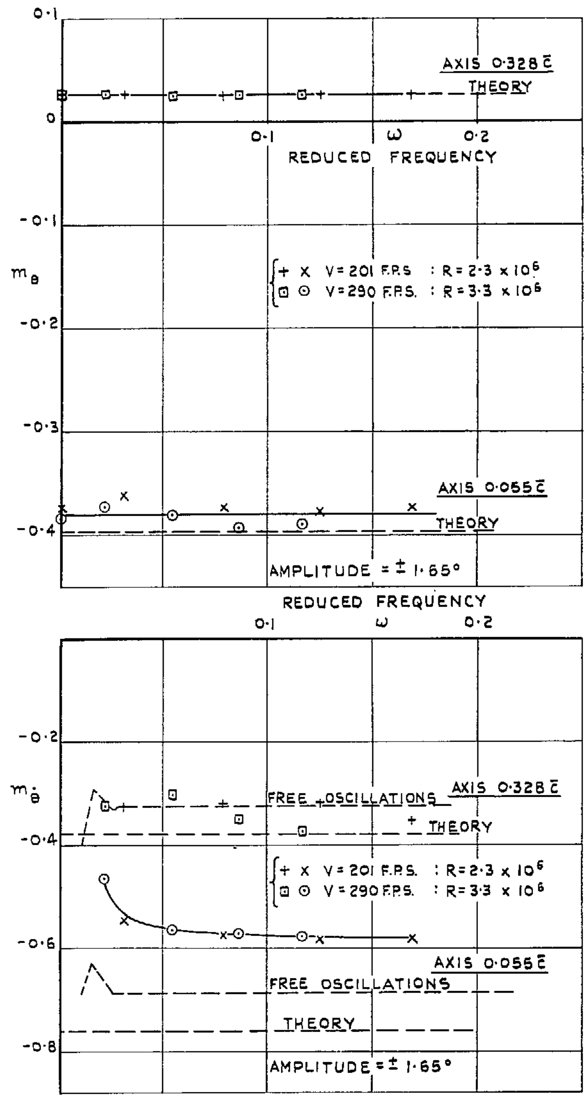

FIG. 13. Values of m_θ and $m_{\dot\theta}$. 5·485-ft span 90-deg delta wing with body. Method of inexorable forcing.

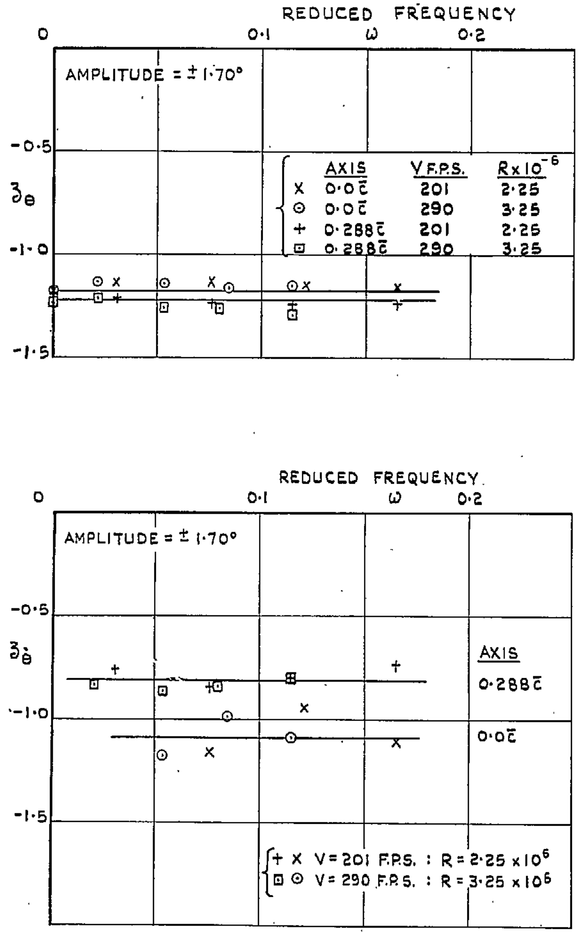

FIG. 14. Values of z_θ and $z_{\dot\theta}$. 60-deg swept-back wing. Method of inexorable forcing.

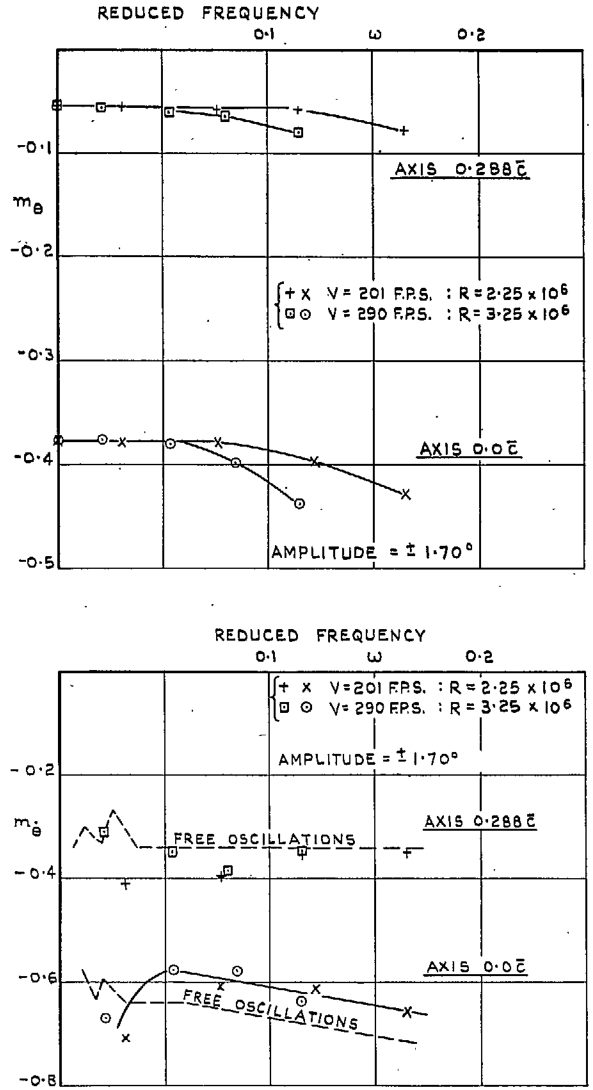

FIG. 15. Values of m_θ and $m_{\dot\theta}$. 60-deg swept-back wing. Method of inexorable forcing.

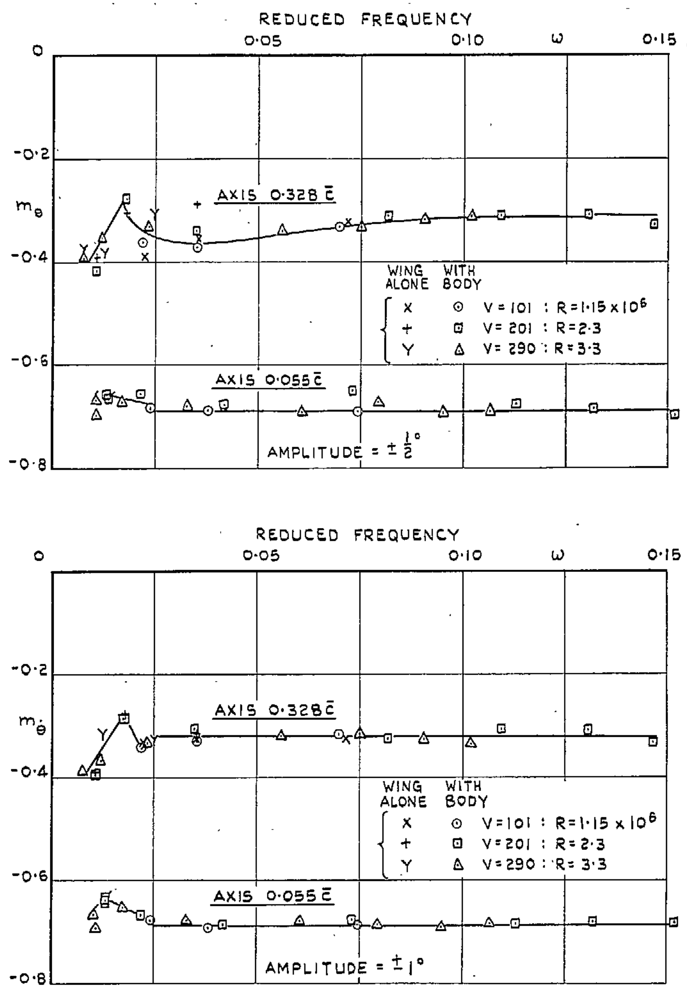

FIG. 16. 5·485-ft span 90-deg delta wing. Damping in pitch for amplitudes $\pm \frac{1}{2}$ deg and $\pm$ 1 deg. Free-oscillation method.

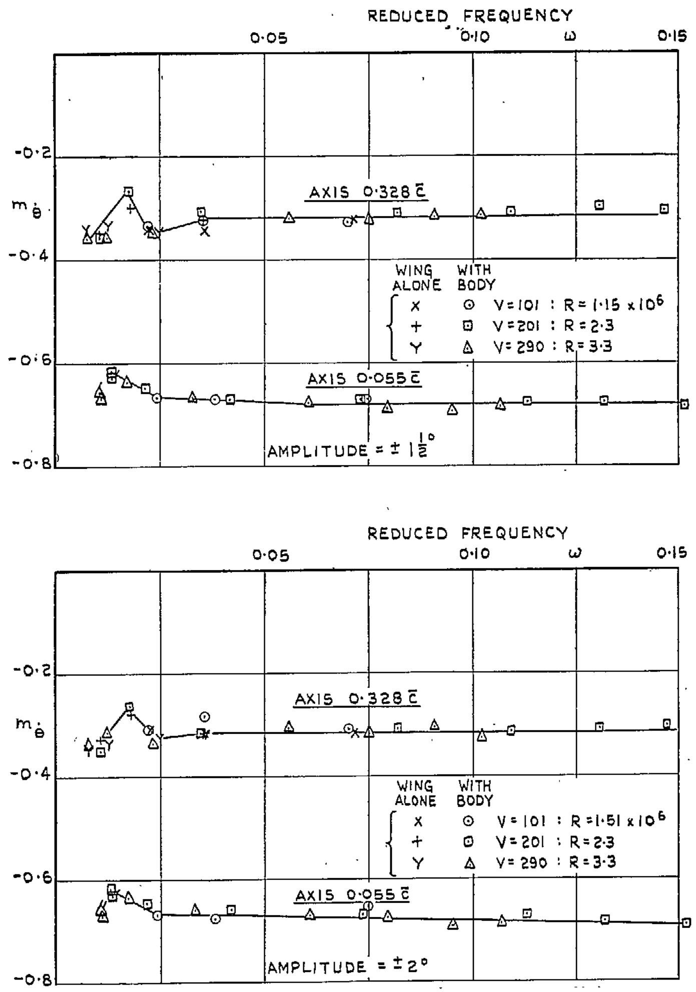

FIG. 17. 5·485-ft span 90-deg delta wing. Damping in pitch for amplitudes $\pm 1\frac{1}{2}$ deg and $\pm$ 2 deg. Free-oscillation method.

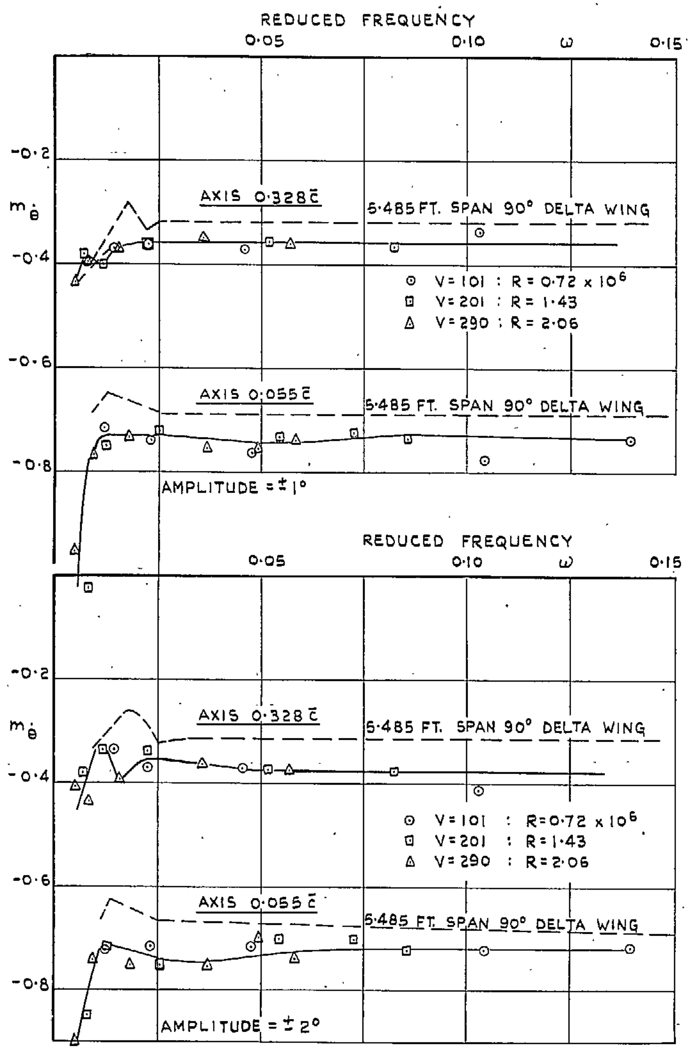

FIG. 18. 3·35-ft span 90-deg delta wing. Damping in pitch for amplitudes ± 1 deg and ± 2 deg. Free-oscillation method.

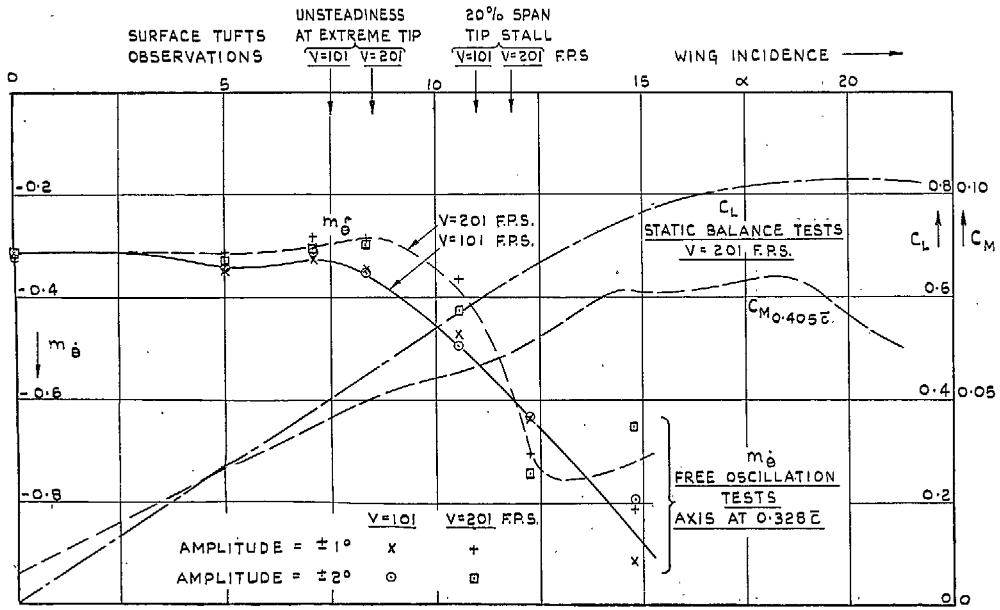

FIG. 19. Variation of damping in pitch with incidence. 5·485-ft span 90-deg delta wing model. No body.

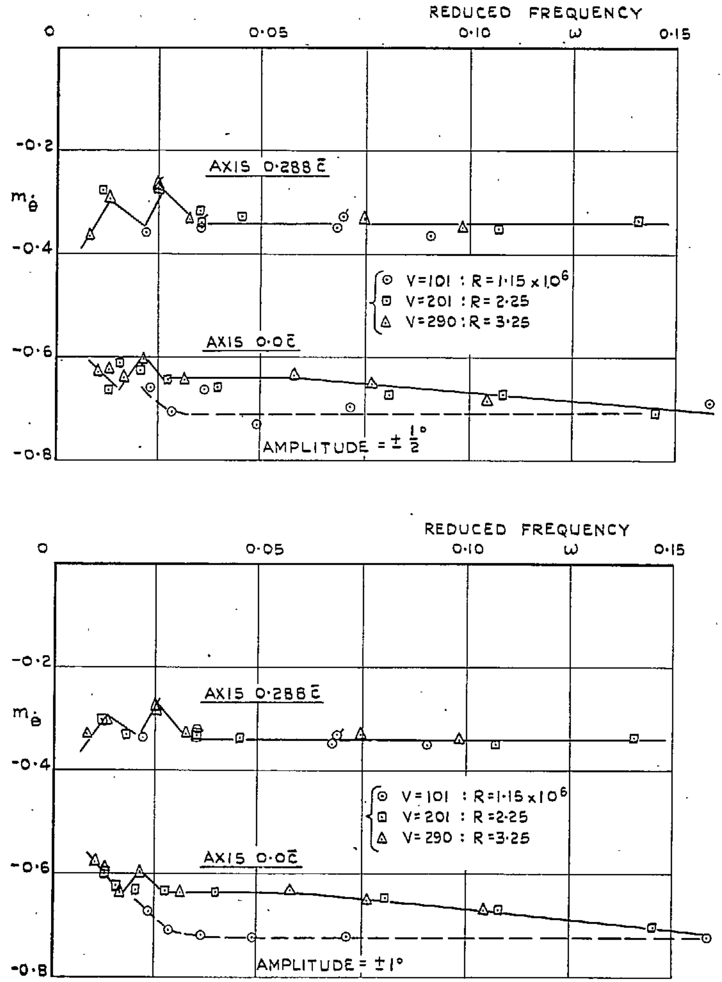

FIG. 20. 60-deg swept-back wing. Damping in pitch for amplitudes $\pm \frac{1}{2}$ deg and $\pm$ 1 deg. Free-oscillation method.

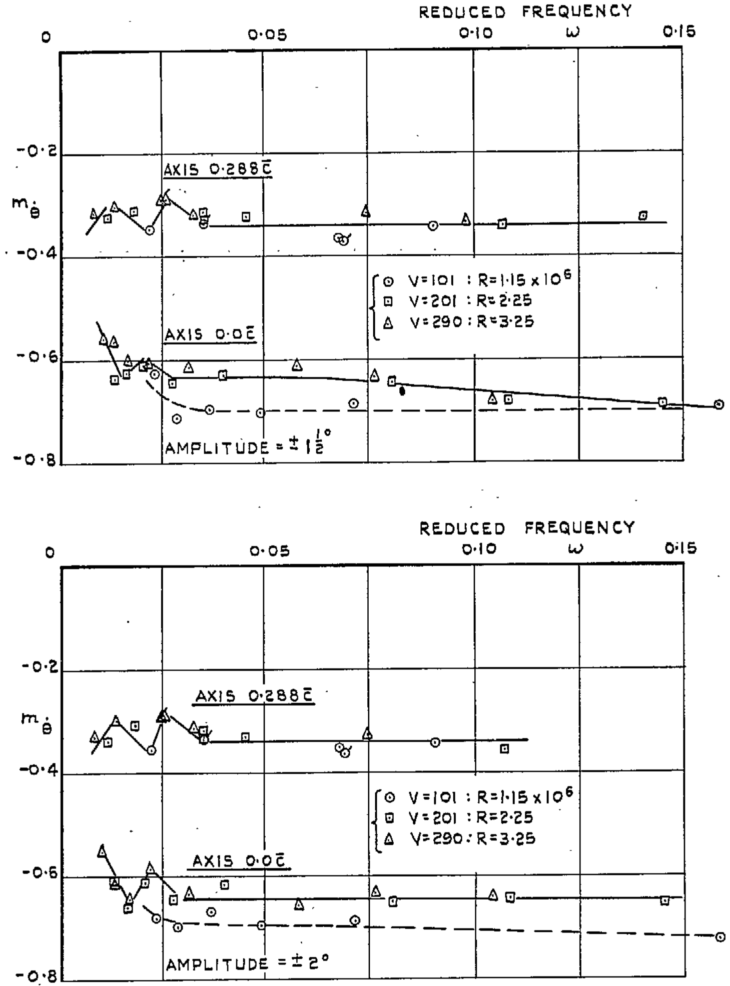

FIG. 21. 60-deg swept-back wing. Damping in pitch for amplitudes $\pm 1\frac{1}{2}$ deg and $\pm$ 2 deg. Free-oscillation method.

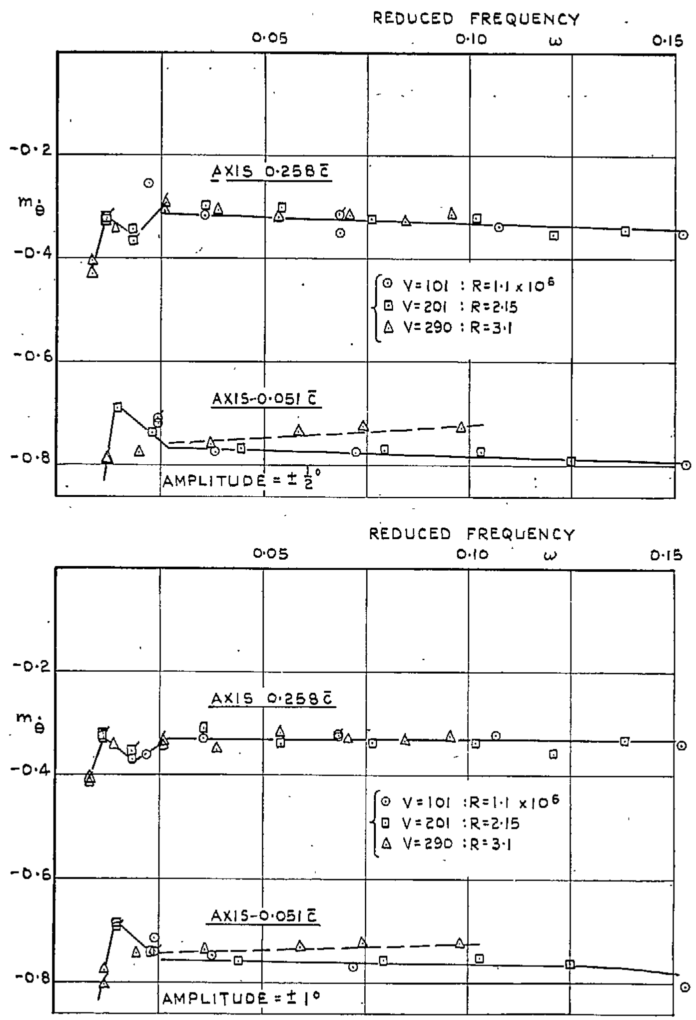

Fig. 22. 40-deg swept-back wing with body. Damping in pitch for amplitudes $\pm \frac{1}{2}$ deg and ± 1 deg. Free-oscillation method.

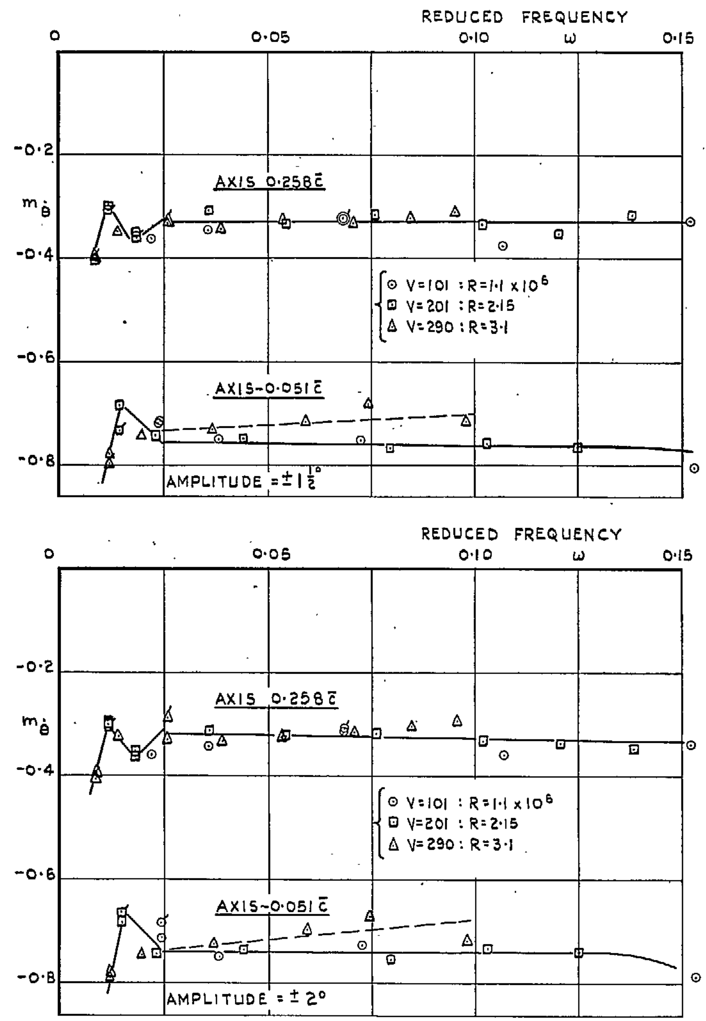

Fig. 23. 40-deg swept-back wing with body. Damping in pitch for amplitudes $\pm 1\frac{1}{2}$ deg and ± 2 deg. Free-oscillation method.

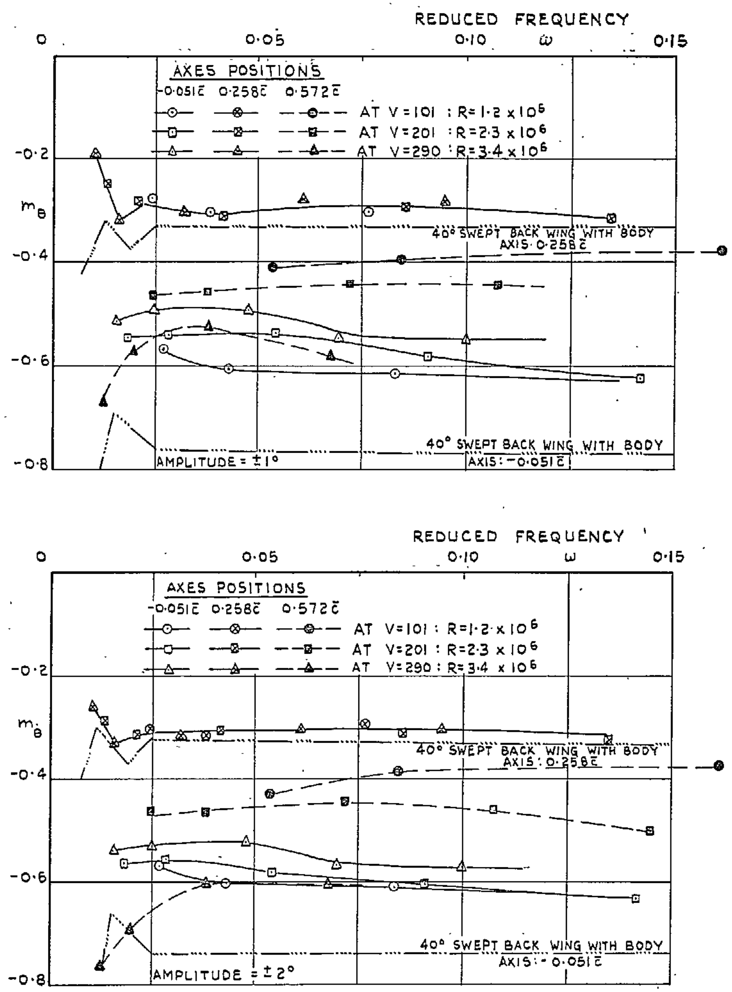

FIG. 24. 40-deg swept-back wing without body. Damping in pitch for amplitudes ± 1 deg and ± 2 deg. Free-oscillation method.

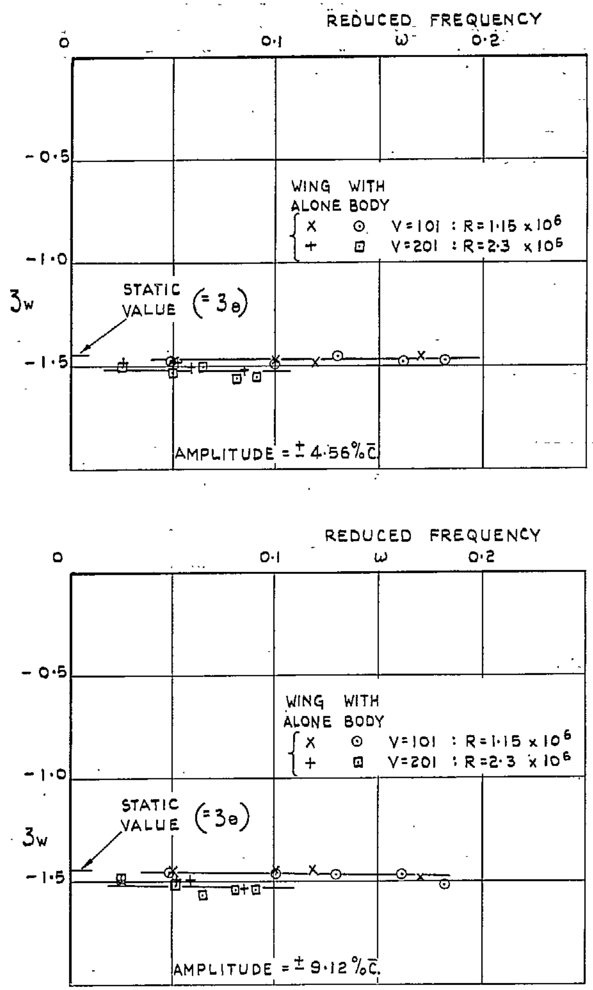

FIG. 25. Values of $\dot{z}_w$. 5·485-ft span 90-deg delta wing. Free-oscillation method.

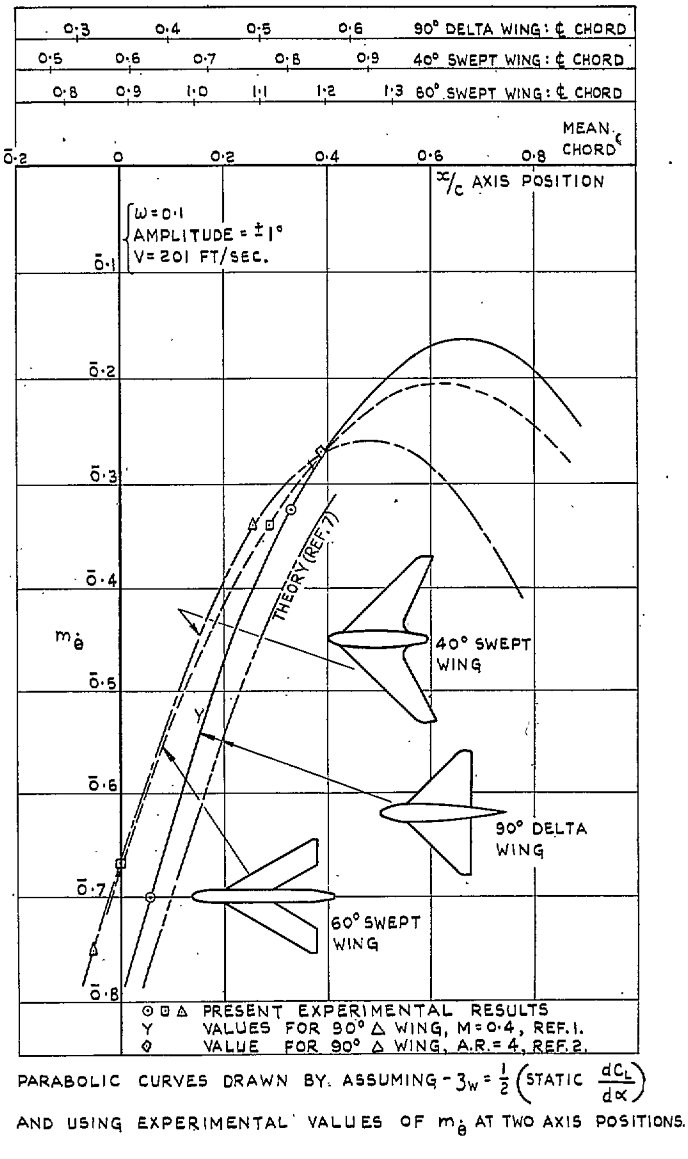

FIG. 26. Variation of $m_{\dot\theta}$ with axis position.

(5028) Wt. 20/9036 K.7 10/57 Hw. PRINTED IN GREAT BRITAIN

Publications of the Aeronautical Research Council

ANNUAL TECHNICAL REPORTS OF THE AERONAUTICAL RESEARCH COUNCIL (BOUND VOLUMES)

1939 Vol. I. Aerodynamics General, Performance, Airscrews, Engines. 50*s.* (51*s.* 9*d.*).
Vol. II. Stability and Control, Flutter and Vibration, Instruments, Structures, Seaplanes, etc. 63*s.* (64*s.* 9*d.*)

1940 Aero and Hydrodynamics, Aerofoils, Airscrews, Engines, Flutter, Icing, Stability and Control Structures, and a miscellaneous section. 50*s.* (51*s.* 9*d.*)

1941 Aero and Hydrodynamics, Aerofoils, Airscrews, Engines, Flutter, Stability and Control Structures. 63*s.* (64*s.* 9*d.*)

1942 Vol. I. Aero and Hydrodynamics, Aerofoils, Airscrews, Engines. 75*s.* (76*s.* 9*d.*)
Vol. II. Noise, Parachutes, Stability and Control, Structures, Vibration, Wind Tunnels. 47*s.* 6*d.* (49*s.* 3*d.*)

1943 Vol. I. Aerodynamics, Aerofoils, Airscrews. 80*s.* (81*s.* 9*d.*)
Vol. II. Engines, Flutter, Materials, Parachutes, Performance, Stability and Control, Structures. 90*s.* (92*s.* 6*d.*)

1944 Vol. I. Aero and Hydrodynamics, Aerofoils, Aircraft, Airscrews, Controls. 84*s.* (86*s.* 3*d.*)
Vol. II. Flutter and Vibration, Materials, Miscellaneous, Navigation, Parachutes, Performance, Plates and Panels, Stability, Structures, Test Equipment, Wind Tunnels. 84*s.* (86*s.* 3*d.*)

1945 Vol. I. Aero and Hydrodynamics, Aerofoils. 130*s.* (132*s.* 6*d.*)
Vol. II. Aircraft, Airscrews, Controls. 130*s.* (132*s.* 6*d.*)
Vol. III. Flutter and Vibration, Instruments, Miscellaneous, Parachutes, Plates and Panels, Propulsion. 130*s.* (132*s.* 3*d.*)
Vol. IV. Stability, Structures, Wind Tunnels, Wind Tunnel Technique. 130*s.* (132*s.* 3*d.*)

Annual Reports of the Aeronautical Research Council—

1937 2*s.* (2*s.* 2*d.*) 1938 1*s.* 6*d.* (1*s.* 8*d.*) 1939–48 3*s.* (3*s.* 3*d.*)

Index to all Reports and Memoranda published in the Annual Technical Reports, and separately—

April, 1950 - - - - R. & M. 2600 2*s.* 6*d.* (2*s.* 8*d.*)

Author Index to all Reports and Memoranda of the Aeronautical Research Council—

1909—January, 1954 R. & M. No. 2570 15*s.* (15*s.* 6*d.*)

Indexes to the Technical Reports of the Aeronautical Research Council—

December 1, 1936—June 30, 1939	R. & M. No. 1850	1*s.* 3*d.* (1*s.* 5*d.*)
July 1, 1939—June 30, 1945	R. & M. No. 1950	1*s.* (1*s.* 2*d.*)
July 1, 1945—June 30, 1946	R. & M. No. 2050	1*s.* (1*s.* 2*d.*)
July 1, 1946—December 31, 1946	R. & M. No. 2150	1*s.* 3*d.* (1*s.* 5*d.*)
January 1, 1947—June 30, 1947	R. & M. No. 2250	1*s.* 3*d.* (1*s.* 5*d.*)

Published Reports and Memoranda of the Aeronautical Research Council—

Between Nos. 2251–2349	R. & M. No. 2350	1*s.* 9*d.* (1*s.* 11*d.*)
Between Nos. 2351–2449	R. & M. No. 2450	2*s.* (2*s.* 2*d.*)
Between Nos. 2451–2549	R. & M. No. 2550	2*s.* 6*d.* (2*s.* 8*d.*)
Between Nos. 2551–2649	R. & M. No. 2650	2*s.* 6*d.* (2*s.* 8*d.*)

Prices in brackets include postage

HER MAJESTY'S STATIONERY OFFICE

York House, Kingsway, London, W.C.2; 423 Oxford Street, London, W.1; 13a Castle Street, Edinburgh 2; 39 King Street, Manchester 2; 2 Edmund Street, Birmingham 3; 109 St. Mary Street, Cardiff; Tower Lane, Bristol 1; 80 Chichester Street, Belfast, *or through any bookseller.*

S.O. Code No. 23-3009

R. & M. No. 3009